IN-20
432260

IAF-98-xxxx

THE ROLE OF THE STRUTJET ENGINE IN NEW GLOBAL AND SPACE MARKETS

A. Siebenhaar and M.J. Bulman
GenCorp Aerojet
PO Box 1322
Sacramento, California

D. K. Bonnar
Boeing Phantom Works
Huntington Beach, California

List Of Tables

List Of Figures

Need Consistent caps and lower case ie for a For in a In

Abstract

The Strutjet, discussed in previous IAF papers, was originally introduced as an enabling propulsion concept for single stage to orbit applications. Recent design considerations indicate that this systems also provides benefits supportive of other commercial non-space applications. This paper describes the technical progress of the Strutjet since 1997 together with a rationale why Rocket Based Combined Cycle Engines in general, and the Strutjet in particular, lend themselves uniquely to systems having the ability to expand current space and open new global "rapid delivery" markets.

During this decade, Strutjet technology has been evaluated in over 1000 tests. Its design maturity has been continuously improved and desired features, like simple variable geometry and low drag flowpath resulting in high performance, have been verified. In addition, data is now available which allows the designer, who is challenged to maximize system operability and economic feasibility, to choose between hydrogen or hydrocarbon fuels for a variety of application. The ability exists now to apply this propulsion system to various vehicles with a multitude of missions.

In this paper, storable hydrocarbon and gaseous hydrogen Strutjet RBCC test data as accomplished to date and as planned for the future is presented, and the degree of required technology maturity achieved so far is assessed. Two vehicles, using cryogenic propane fuel Strutjet engines, and specifically designed for rapid point-to-point cargo delivery between Pacific rim locations are introduced, discussed, and compared.

1.0 Introduction

The premise of this paper is: "Low Cost Transportation Will Enable New Markets", or new global and space markets can be opened if government and industry leaders subscribe to a change in the decades-old mind set about what is "necessary" to operate launch vehicles[1].

Let's look at system development cost. The shuttle orbiter took about $12 billion to develop, and at eight, or fewer, flights per year the cost to launch payloads amounts to $10,000/lbm just to pay for the development cost. In contrast, a new commercial aircraft, like the Boeing 777, with a development cost of $7 billion amortizes this investment over its lifetime with a payload cost of about $10/lbm. Obviously, the former is not a viable basis for business, and the latter is very good business. When looking at the systems operating cost the situation does not improve.

One would assume that today's reusable launch vehicle community (RLV) would endorse the airline approach, but the fact is that most commercial reusable vehicles are still being built more like space shuttle orbiters than commercial aircraft. In order to bring the cost down, these vehicle are designed for a life of 50 to 100 flights, too meager an improvement, because at the optimistically projected payload cost of $1000/lbm the production cost can just be covered, and a higher price must be charged to cover operating cost and profits. If these systems could be designed for, let's say, 1000 to 2000 flights per life, the payload cost could be reduced to $10 to 100/lbm, and new rapid global reach and orbit markets could be realized[2].

The key to such a capability is the abandonment of the extremely high power density of the classical rocket as the sole means of propulsion. Low cost systems need engines and subsystems capable of operating for thousands of hours between overhaul, have built-in self-checking capabilities, and are designed for quick replacement in the field without disturbing other systems. The Aerojet Strutjet engine[3, 4] is an engine with the potential to provide simultaneously higher performance, more safety, and higher reliability than rockets. An investment in its high-reliability design will quickly pay off in faster turn-around times, higher utilization of each vehicle, customer confidence, and greatly reduced insurance rates. Traditionally, rockets must be built with small margins because

inherently high mass fraction rocket vehicles require all the performance achievable. This strategy is acceptable for expendable systems, but it leads to a major downfall in the attempt to adopt it to reusable systems. Here robustness, obtained in exchange for performance, is the key parameter from which all desirable attributes of low cost through reusability can be derived. The point in case is illustrated for space access missions in Figure 1 which relates lower engine replacement cost to the 80% reduced thrust requirement, and lower maintenance and operating cost to higher structural margins and redundancy. Both these savings result from the increased specific impulse of RBCC engines and the associated reduction in takeoff and dry mass.

Future markets lie beyond space access. If RLV technology is brought to bear to hypersonic transport of rapid delivery systems for first cargo and possibly later passengers between key traffic centers, the RLV traffic will jump to thousands of flights per year. This will require a more airport-like layout of launch operations including noise mitigation, air-traffic control, and, because of high acquisition and storage cost, a departure from liquid hydrogen as the main fuel. Hydrocarbon fuels, e.g. cryogenic methane or propane, or other kerosene based jet fuels will be the propellants of choice.

The key to successful business is a vehicle/operations/infrastructure system design focusing from the outset on the efficient achievement of high flight rates. Structuring the system to expand rapidly to fill new markets will have a large economic advantage over today's approach with systems designed for traditional launch rates and subsequently applied to a demand-elastic market.

This paper describes briefly in Section 2 the space access version of the Strutjet engine, and provides in Section 3 a status of Strutjet RBCC test data addressing both storable hydrocarbon and gaseous hydrogen fuels. In Section 4 an assessment of the current maturity level of required Strutjet technology levels is made. Finally, Section 5 introduces a preliminary study of an rapid cargo delivery system capable of delivering payloads from the United States to various locations on the Pacific rim. This study is to be viewed as an appetizer to stimulate future further exploration of these potential capabilities of RBCC propulsion. Section 6 sums up the overall paper content, and Section 7 provides the relevant references.

2.0 Space Access Strutjet Engine Description

The Aerojet Strutjet engine is a member of the rocket based combined cycle (RBCC) class of engines with several new technologies and innovations. Many of these technologies are also of far reaching interest in other propulsion schemes. The Strutjet engine operates all of the cycles with liquid hydrogen (LH2) for fuel, and liquid oxygen (LOX) and atmospheric air as necessary for combustion of fuel.

The name *Strutjet* is derived from the use of a series of struts in the front part of the engine flowpath. The struts serve a number of functions in the engine, including compression of incoming air, isolation of combustion from air inlet (that is, as an isolator), fuel distribution and injection, ram/scram combustion, and rocket-thruster integration in the different modes of engine operation. The struts provide efficient structural support for the engine. The struts thus form a key element in the engine.

The Strutjet engine is in principle, a single engine configuration with three propulsion elements, namely rocket, ramjet, and scramjet in its five mode operation. The elements are highly integrated in design and function. The Strutjet differs from other RBCC designs in the higher degree of functional integration of various engine components which results in a shorter, higher thrust-to-weight engine with good performance. The specific impulse of the Strutjet engine is characteristic of other known airbreathing engines without the thrust-to-weight penalty of having separate propulsion systems for different flight conditions.

The Strutjet engine concept is founded on obtaining specific impulse, I_{sp}, higher than that of a rocket, a better thrust-to-weight ratio (F/W_e) than an all-airbreathing engine, and a substantial reduction in vehicle gross take-off-weight. Thus along a typical trajectory of a single stage to orbit (SSTO) vehicle the mean I_{sp} for the Strutjet is estimated to be 586 sec, while the conventional hydrogen-oxygen rocket provides I_{sp} of only 425 sec. In comparison, the mean I_{sp} for an all-airbreather such as the USA

National AeroSpace Plane (NASP) was estimated to be 755 sec. A SSTO-type all-rocket may yield F/W_e equal to 80:1 and a NASP-type SSTO all-airbreather, about 6:1. Using current state-of-the-art technology, a hydrogen fueled Strutjet can be built with F/W_e of 35:1; however, for the sake of increased engine robustness, low earth orbit missions can still be achieved with F/W_e values as low as 25:1.

Figure 2 provides a schematic of the Strutjet and identifies the different elements in the combined cycle engine. The propulsion subsystems are integrated into a single engine using common propellant feed lines, cooling systems, and controls. The air inlet along with the struts, the combustion sections, and the nozzle make up the main engine flow path. An isometric view of a typical RBCC Strutjet engine is given in Figure 3.

The variable geometry inlet incorporates two engine ramps, that maximize air capture and control compression as required by the engine. The inlet combines effective forebody precompression with strut compression. This results in "soft start", low spill drag, and good capture and recovery efficiencies. The "soft start" is a result of the increased openness of the inlet on the cowl side, which causes a gradual decrease in spillage with increasing Mach number. This, in turn, provides smooth increases in captured air mass flow and pressure recovery. The inlet geometry and the changes in contraction ratio as a function of flight Mach number are shown in Figure 4. Past the cowl lip, at low speeds, the flow area between two adjacent struts remains constant; the strut section serves as an inlet combustor isolator during ducted rocket and ramjet mode. At higher speeds ($M \approx 5$) the inlet ramps are deployed to increase the engine contraction and performance.

Above Mach 6 the scram mode is the most efficient and the diverging isolator duct between the fully contracted inlet throat and the rockets is used as the scram combustor. During this mode of operation the variable nozzle geometry adjusts the scram combustor flowpath into a continuously diverging configuration.

The ram combustor used at speeds up to Mach 6, is located aft of the strut rockets. This combustor provides enough area to permit stoichiometric subsonic combustion at low speeds.

The Strutjet variable geometry nozzle is a simple flap used to control subsonic combustion pressure to create the optimum thrust as dictated by operating mode and flight Mach number. This nozzle flap is the principle control in the transition to the scram mode. By opening the nozzle flap up at approximately Mach 6, the combustor pressure drops and the flow remains supersonic through the combustor.

The overall Strutjet engine propellant flow is illustrated in Figure 5. As shown, there are three subsystems: (i) the hydrogen and oxygen fuel tanks, turbopumps feed system and powerhead; (ii) the strutrocket and fuel injection assembly, and (iii) the engine structure and cooling system. Both the strut rocket and the engine structure are operating in the thermal and combustion gasdynamic environment.

Fuel rich gases generated in the fuel gas generator (FGG) drive the hydrogen turbine, and are subsequently injected into the engine internal air stream at selected locations through base-axial, aft, and forward injectors. The selection depends on the engine operating mode, and is accomplished through appropriate valving. Hydrogen gas is also used to cool the rocket chambers (the figure including schematically only one) and the engine structure before injection into the combustor section. In the expander cycle, hydrogen heated by the engine structure bypasses the preburner and drives the turbine in an expander cycle.

The oxygen side of the propellant system is only active during rocket operation, and operates (always) in a stage-combustion cycle. The oxygen rich turbine drive gases are generated in the preburner (OPB) through the burning of a small amount of hydrogen and all of the oxygen flow, prior to injection into the rocket chambers.

The table shown at the bottom in Figure 5 includes four attributes for each of the five operating modes, and indicates graphically the required settings for a particular mode:

(i) selected power cycle in the oxygen and hydrogen supplied,

(ii) amount of rocket propellant flow,

(iii) amount of hydrogen injected into the air stream, and

(iv) settings of the inlet and nozzle variable geometry.

Along a typical SSTO ascent trajectory a Strutjet operates in five modes with smooth transition between modes:

I. ducted rocket operation for takeoff and acceleration through the transonic speed regime into the supersonic region;

II. ramjet operation from Mach 2.5 to about 6;

III. scramjet operation from Mach 6 into the hypersonic speed range up to Mach 10;

IV. scram /rocket operation from Mach 10 to low vacuum conditions; and

V. ascent rocket from low vacuum operation up to orbital speeds.

3.0 Available Hydrocarbon and Hydrogen Test Data and Planned Future Test Activities

The overall test program, accomplished to-date or planned for the near future, may be divided into two groups: (i) missile propulsion tests using storable hydrocarbon fuels, and

(ii) space launch propulsion tests using gaseous hydrogen fuel.

3.1 Storable Hydrocarbon System Tests

Aerojet performed a test program which parametrically examined the RBCC Strutjet propulsion system from Mach 0 to 8 over the altitude range from 0 to 100,000 ft. The tests were carried out in the context of a long range missile, two configurations of which are shown in Figures 6 and 7. However, the test results obtained during this campaign are equally applicable to a launch system Strujet like the one described in Section 2. In over 1000 hot fire & inlet tests a number of achievements were realized:

- The strut inlet provides excellent air capture, pressure recovery, and unstart margin.
- The integration of compact high chamber pressure rockets using gelled hypergolic & cryogenic propellants into a strut is structurally and thermally feasible.
- A fixed engine flowpath geometry suitable for all modes of operation can be established providing adequate thrust and specific impulse to accomplish mission objectives.
- Static sea level thrust augmentation of 13% can be achieved due to the interaction of air ingested with the fuel-rich rocket plume.
- The ducted rocket thrust increases with increased flight Math number. At Mach 2.85 and altitude 20,000 ft the thrust increase is over 100%. And, at Mach 3.9 and altitude 40,000 ft. the ramjet thrust exceeds the rocket sea-level thrust by 19%.
- Dual-mode operation of the ram-scram combustor with a thermally choked nozzle is feasible.
- Efficient combustion at high altitude and with short combustors is possible with hypergolic pilots. Combustion efficiency of 90% can be demonstrated with a combustor only 30 in. long at Mach 8 conditions.

Inlet Tests

As part of the first Strutjet inlet test program, a subscale inlet model, shown in Figures 8 and 9, was constructed to evaluate design options for the freejet engine inlet design. Prior to this testing, engine/vehicle performance was based on extrapolating the performance of the inlet from the literature (mostly the work of NASA LaRC). The objectives of the inlet development was to define a missile like inlet that would interface with the hydrocarbon combustor which up to this point had only been tested in a direct connect

configuration. A very conservative design was selected that had no internal contraction to assure starting. This inlet was found to start at all tested Mach numbers (4-6), and as shown in Figure 10, it produced excellent pressure rise. As predicted, it exhibited low energy flow near the body side of the flowpath, a phenomenon which had to be dealt with in the subsequent freejet tests via matching the fuel injection with the actual air flow distribution.

Ducted Rocket Tests

In these tests, each strut contained three water-cooled gelled IRFNA and MMH propellant rockets, as shown in Figure 11. The injector pattern consisted of 36 pairs of fuel and oxidizer elements arranged in concentric rings, the outermost ring providing fuel film cooling to the chamber. The chamber geometry is shown in Figure 12. The characteristic parameters of the injector are summarized in Table 1.

As illustrated in Figure 13, the rig representing the Strutjet engine was designed as a sandwich with hinged side wall sections. The duct section housing the strutrocket had a fixed geometry of 4.0 in by 6.6 in. The isolator section in front of the strut duct could be connected to either a bell mouth for a static test or a hydrogen fueled vitiated air heater. Two struts were mounted in the strut duct, dividing the flowpath to the inlet into three channels.

In the sea level static ducted rocket tests the isolator section in front of the strut duct was fitted with a calibrated bell mouth. The duct geometry was varied to determine the configuration yielding the maximum thrust. Sensitivities of rocket chamber pressure, mixture ratio, and rocket nozzle expansion ratio were also established. As shown in Figure 14, thrust enhancement was a strong function of the ram burner throat area and a somewhat weaker function of the ramburner geometry. With a duct geometry of 3°–3°, 13% more thrust was obtained than for the reference rocket in a particular test with a throat area of 32 in^2. Data analysis indicated that oxygen content of the inducted air was completely consumed in approximately 8 in. from the rocket baseline. Considering the influence of chamber pressure, operation at 2000 psia generated more thrust than operation at 1600 psia; however, airflow and thrust augmentation were reduced by 19% and 3%, respectively. The area ratio of 11:1 generated 12% higher induced air flow and

6% more thrust than the lower area ratio of 5:1. Finally, it was observed that greater air flow and higher thrust result from operation at higher mixture ratios due to reduced thermal choking resulting from the afterburning scheme.

In the direct-connect ducted rocket tests which allow evaluation of the engine under flight trajectory conditions, the isolator section in front of the strut duct was connected to a hydrogen vitiated air heater with a Mach 2 nozzle. The duct geometry which, in the static tests, provided the maximum take-off thrust augmentation was maintained in these direct-connect tests. Measuring the duct pressure and assuming a particular inlet performance, allows for the determination of flight altitude and Mach number simulated in a given test. Figure 15 shows the thrust obtained in the ducted rocket and ramjet tests. The left branch of the figure depicts the thrust of the ducted rocket without additional fuel injection, and the right branch, that of the ramjet without rocket operation. The ducted rocket tests were conducted under fuel-rich conditions, the excess fuel sufficient to support 10 lbm/sec of air flow. The simulated trajectory provides 10 lbm/sec of air at approximately Mach 1.5. Tests beyond Mach 1.5 were thus "lean" on an overall engine stoichiometric basis. Auxiliary fuel injectors could be used to increase the engine thrust. The peak thrust is seen to occur at a simulated altitude of 23,000 ft and Mach 2.85, with 31 lbm/sec of air being supplied to the engine. The peak thrust is over twice the bare rocket value, representing better than 100% thrust augmentation.

Direct Connect Ram and Scramjet Tests

The ramjet tests were conducted at Mach numbers of 2 and higher without rocket operation to optimize ramjet injector performance. The primary ramjet test variable, other than the injector parameters, was the fuel of choice. In support of the strategy for minimizing heat load and hot spots, the main emphasis was on achieving a short combustor length.

In the scramjet operating regime three test series were conducted:

In the first tests the scramjet geometry was explored and high combustion efficiency with a fixed geometry over the Mach number range of 2 to 8 were demonstrated. Mach 2 and

4 tests were conducted with JP-10 fuel. The Mach 8 tests simulated the effect of regeneratively heated fuel by using ethane instead of JP-10.

In the second test series, the tests conducted with ethane were repeated with JP-10 fuel, using a slightly modified duct geometry, namely the first 12 in. downstream being of constant area followed by a 2° double-sided expansion over the remaining duct length. Auto-ignition was not achieved; however, when pilots were utilized for ignition and flame sustaining, stable combustion at 95% efficiency was observed. As shown in Figure 16, the test duplicated, in essence, the performance previously achieved with ethane, with only the slight change in duct geometry. The Strutjet design used in these tests provided for a contact pilot at each injection point of the hydrocarbon ramjet fuel. This pilot derives its energy from the combustion of small amounts of the gelled rocket propellants which are injected and burned upstream of the hydrocarbon injection. Due to the hypergolic nature of the employed rocket propellants the pilots act initially as igniters and subsequently as flame sustainers, allowing flight at high Mach numbers and high altitudes. The demonstration of this feature is verified by the data presented in Figure 17. At a simulated flight condition of Mach 4 and 40,000 ft of altitude JP-10 was ignited by the pilot resulting immediately in a thrust increase of about 2,000 lbf. Combustion and thrust production were sustained as long as the pilot stayed on. When turned off, the combustion ceases and thrust collapses.

The third test series was in support of the first freejet tests of the Strutjet engine to be conducted by NASA Lewis Research Center at their Hypersonic Test Facility (HTF) in Plum Brook. This facility has the capability to run simulated freejet flight conditions at Mach numbers of 5, 6 and 7 with a dynamic pressure of 1,000 psf. All previous strutjet direct-connect tests, were conducted at a dynamic pressure of 2,000 psf or higher. In addition the Strutjet testing had only been conducted at simulated flight conditions of M = 0-4 and 8. For the sake of risk reduction, additional direct-connect tests were conducted at Mach 6 and 7 at the reduced dynamic pressure. Figure 18 shows the test configuration and also the duct pressures achieved. These tests used the initial combustor divergence found efficient in the ducted rocket/ramjet test series. By properly staging the pilot and the unheated liquid JP-10 injection, good combustion efficiency was achieved

without reducing the duct divergence. This was a significant accomplishment since the employed engine geometry proved to be satisfactory for operation from Mach 0 to 8.

Freejet Tests

The freejet engine shown in Figure 19 was designed constructed by Aerojet, delivered to and tested at Plum Brook. Tests were conducted with the identical fuel injection strategy used in the Mach 7 direct connect tests discussed above. These tests demonstrated inlet starting, fueled unstart with a large forward fueling split followed by inlet restart with shifting the fuel aft and substantial thrust increase. Figure 20 shows the internal pressure profiles and compares the freejet to the inlet data. Figure 21 shows the differential thrust produced as a function of the fuel flow. The slope break at an equivalence ratio of 0.55 is notable. This is the expected result of the non-uniform airflow distribution in the isolator. In the final test at HTF, the fuel injection distribution was shifted to better match the airflow. Unfortunately the facility experienced a hot isolation valve failure prematurely ending the test campaign.

3.2 Gaseous Hydrogen System Tests

All hydrogen systems considered for the Strutjet engine use cryogenic hydrogen. This hydrogen is used to cool the engine regeneratively. During this cooling process the hydrogen converts from a cryogen to a gas. All combustion related processes of the Strutjet engine will then use gaseous hydrogen as a fuel. Therefore, all combustion related tests were conducted with gaseous hydrogen. The tests described here were executed as part of the Advanced Reusable Technology program sponsored by NASA MSFC and supported by Aerojet with the objective to demonstrate the technology of the hydrogen fueled RBCC Strutjet engine previously described in section 2.

Inlet Tests

The previously shown Figure 4 illustrates schematically the air flow path on the vehicle underbody. Forebody compression reduces the inlet approach Mach number. For example, if the freestream Mach number is 6.0 then the approach Mach number is reduced to 4.2. A model of the inlet-isolator test article is shown in Figure 22. The inlet model accurately simulates the inlet from just upstream of the struts all the way through to the ram combustor. Geometrical similarity between the full-scale SSTO vehicle,

capable of delivering 25,000 lbm payload to the International Space Station, and the subscale test article is maintained. The model is 6.8% scale of the full size inlet. The inlet is preceded by a plate simulating the vehicle forebody boundary layer. While the full-scale engine contains 8 to 16 struts and two sidewalls, the test article is composed of two struts and two sidewalls. In the model, the sidewalls are positioned to represent the symmetry plane between struts, thereby fully simulating flow around and between struts. The full-scale engine has two bleed locations, a forebody and a throat bleed. In order to adjust for the non-linear scale effects the inlet subscale model has an additional strut bleed which removes excess boundary layer build up on the sidewalls. A throat plug is used to simulate combustion pressure increase.

The testing of this inlet in the NASA LeRC supersonic wind tunnel provided excellent results. Tests were performed over simulated flight Mach numbers from 3.6 to 8.1. The inlet started at all Mach numbers, and exhibited unstart margins of over 20% in ramjet and 100% in scramjet modes. With forebody spill excluded, engine capture efficiency exceeded 90%, which is remarkable, considering the wide operating range and large unstart margin realized with this inlet. The inlet started easily at all Mach numbers and generated excellent pressure rise, as shown in Figure 23.

Strut Rocket Tests

Aerojet and NASA Marshall Space Flight Center completed proof-of-concept testing on a new strut rocket injector element developed to enable operations under the unique strutrocket conditions. This element has been incorporated into the design of six subscale strut rockets for ducted rocket testing.

The primary objective for a part of these tests was to demonstrate the performance and durability of a new injector which had been designed to maximize thruster efficiency while minimizing thruster length. The injector design ensures efficient mixing of the propellants within the chamber by employing an impinging element design and by utilizing a refined element pattern: 18 elements on the 0.5 inch diameter injector face. Figure 24 shows the injector firing in a single chamber in tests at Aerojet. Thermocouple data verified that the temperature of the injector face was within the limits predicted for the design. Post-test visual inspections of the test articles indicate that the injectors

suffered virtually no erosive or other damage related to excessive face temperatures. Scanning electron microscope images of single elements and single orifices produced at MSFC are particularly encouraging. The data obtained during 16 hot-fire tests extend over the ranges indicated in Table 2:

Subscale strutrockets were fabricated and check out tests were complete. In these tests the propellant, coolant and ignition sequences required for RBCC operation were developed, and unaugmented rocket thrust was determined to establish a reference for subsequent combined cycle testing. Aerojet is also currently fabricating a full scale strutrocket using the same injector element. During the testing of this test article laser diagnostics will be used to measure the fuel distribution in the rocket exhaust for various design and operating conditions.

Direct Connect Ram & Scramjet Tests

Aerojet successfully demonstrated the efficiency of this fuel injection strategy at Mach 6 and 8. Figure 25 shows one of the test strut assembly for the direct connect campaign. Two struts are shown installed in the test rig in Figure 26.

Three test series were conducted: ram and scram tests at simulated Mach 6 flight conditions, and scram mode tests at Mach 8 conditions. High performance was achieved in all three test series in only 27 tests. A key to this success was the use of the cascade scram injectors in the forward location. These low drag supersonic injectors are shown in Figure 27. The fuel split for each mode and Mach number was determined by the inlet tolerance to the combustion pressure rise. Excellent performance at stoichiometric conditions was demonstrated at each Mach number and mode tested, by simple adjustment of the fuel flow to each of the three injectors. The data indicated that the performance of the cascade injector was even better than expected. Evidence of over-penetration suggested additional improvement can be made by increasing the number of cascades from 4 per strut side to 5 or more. This can be expected to increase the combustion rate and permit even shorter, lighter engine designs.

Planned Tests

In the first two tests strutrockets, shown in Figure 28, will be installed in the direct connect duct to explore the performance in the Scram/Rocket and Ascent/Rocket Modes. A second pair of strutrockets will be installed in the new freejet engine and tested first under sea level static conditions and then in the ducted rocket and ramjet modes. Of particular interest is the transition from ducted rocket to ramjet mode at a flight Mach number of about 2.5. Freejet test hardware is shown in Figures 29, 30, and 31, showing the inlet variable geometry, the integration of the strutrockets into the combustor, and the overall cross section of the flowpath. Comparison between Figures 4 and 31 reveal the operation of the inlet variable geometry. The nozzle flap shown in Figure 31 is integrated in the test hardware on the body side of the engine for test arrangement purposes; in the flight engine the nozzle flap will be on the opposing cowl side.

The contemplated test facility has the capability to provide accelerating test conditions. This allows tests to begin at one Mach number and sweep continuously to a higher one while simultaneously matching pressure and enthalpy. Using this facility, it will be possible to demonstrate the ducted rocket to ramjet and the ram to scram transitions.

4.0 Maturity of Required Strutjet Technologies

The maturity of RBCC engines is best defined in terms of a 'Technology Readyness Level" (TRL) as defined by NASA. The following assessment is as of Summer 1998 relative to a TRL of 6 which requires technology demonstration in a relevant environment be it simulated on the ground or actually flown. Table 3 categorizes various aspects of an RBCC engine into the degree of maturity relative to TRL 6.

It is evident from the table that a large amount of development must be accomplished before a TRL of 6 is achieved for the Strutjet RBCC engine. With this assessment in mind, it may not be prudent to risk at this point in time the commitment of large amount of resources towards the exclusive RBCC approach to achieve low cost access to space. For near term applications alternate approaches, like further maturation of all rocket propulsion, should be employed. However, the potential of RBCC engines is so

overwhelming that it is also not prudent to casually dismiss the opportunity to exploit the RBCC option.

5.0 Description Of A Rapid Cargo Delivery System

Mission Description - For the rapid cargo delivery systems (RCDS) considered, it is assumed that the concept of a multy hub concept is employed. Between hubs, which typically would be separated by oceans, the cargo is hypersonically transported using the RCDS; to and from hubs, the cargo is flown via subsonic aircraft. If hubs are located near an ocean or in areas of low population density the hypersonic portion of the mission can be accomplished with ground launched RCDS. If these hub conditions are not given, air launched RCDS vehicles can be carried on top of large transport aircraft to environmentally feasible launch sites and then released. Since the entire concept is only economically more feasible if very high launch rates are considered, the environmental impact resulting from combustion exhaust gases and noise generation will have a very strong influence. In order to bring the operating cost down, hydrogen fuel has to be abondoned. The fuel of choice, and the one further pursued in this paper, is cryogenic propane. It is anticipated that this fuel will simplify the fuel supply infrastructure, and fuel loading operations.

The baseline missions selected for cargo delivery are summarized in Table 4. Since the emphasis of this study is on Pacific rim markets two main Western United States based hubs are considered: Los Angeles and Anchorage. The primary destination hubs, shown in Figure 32, are in other Pacific rim countries, except for a hub in Kirma, Sweden, which can easily be reached via a polar route and could open up the European market. The baseline RCDS vehicle designs are sized to cover the maximum range needed; shorter range hubs can be accommodated using the same vehicles through propellant off loading. The maximum ranges to be achievable in this mission model are about 7620 mi or 14,111 km, one being Los Angeles to Singapore, and the other, with an equivalent range, Anchorage to Perth, Australia.

RBCC Engine Model - The baseline engine model used in the following vehicle designs and trajectory simulations uses liquid oxygen (LO_2) and liquid propane (LC_2H_8) with a mixture ratio of 3. This engine is in principle very similar to the engine previously shown in Figures 2, 3 and 4. A qualitative comparison of the predicted performance of the hydrogen and the propane Strutjets in terms of specific impulse is given in Figure 33. Again, the ducted rocket mode provides some enhanced impulse over the pure rocket mode up to Mach 2.5, where the ramjet mode initiates. The scramjet mode carries out to a cutoff at the transition Mach (M_T) number of 10. The specific impulse is the "cowl-to-tail" (no forebody drag) engine performance. In the simulations, the effective Isp is reduced by the vehicle/engine atmosphere drag as shown in Figure 34. At the transition Mach number the engine will first operate in the combined scramjet/ascent rocket mode, and then gradually tranition into the ascent rocket mode for the remainder of the burn. After burnout the Strutjet engine is shut down and not used anymore for the remainder of the mission because the vehicle will enter a glide phase and land at the target hub unpowered..

The RBCC engine thrust-time history for the ground-launched vehicle is shown in Figure 35. This thrust profile addresses all modes of power-on operation. The selected capture area of the installed Strutjet engine is 255 ft^2, and during the airbreather mode of operation the dynamic pressure is assumed to be 2,000 psf. The ducted rocket mode is terminated at an altitude of about 30 kft. The ascent-rocket or pure-rocket mode is initiated at an altitude of 98 kft, and burnout occurs at an altitude of 180 kft.

Ground-Launched Vehicle Design Baseline - While an earlier paper[4] described the LO_2/LH_2 RBCC orbital vehicle design trades for carrying 25 klbm to the International Space Station orbit, this paper contains a baseline LO_2/ LC_2H_8 vehicle design of a ground launched (horizontal takeoff/horizontal landing) rapid cargo delivery system (RCDS-GL) sized to deliver 5 klbm to various bases, primarily to Pacific rim locations. This baseline vehicle is compared to the Space Shuttle and the previously established orbital RBCC vehicle in Figure 36, and shown in more detail in Figure 37. The gross liftoff mass of this RCDS-GL is about 477 klbm, and the dry mass is estimated to be 79 klbm; usable

propellant is about 373 klbm as shown in the table contained in Figure 37. This vehicle design provides 29 klbm for runway propellant, which leaves the ignition mass at 506 klbm. This vehicle is about 110 ft long, has a wing span of 50 ft, and requires two RBCC engines each with 143 klb thrust to achieve a vehicle lift-off thrust-to-weight ratio of 0.6:1. The cargo bay of 10 x 20 ft is compatible with a typical 5,000 lbm cargo volume. The RBCC engine thrust-to-weight is assumed to be 43:1, which due to the use of the higher density propane fuel is substantially higher than that for the hydrogen engine. The vehicle total velocity is sized to achieve 26,900 fps, which includes an axial maneuvering velocity reserve of 1,000 fps for landing. The reaction control system (RCS) velocity of 200 fps is sufficient for exoatmospheric attitude control while gliding down from 200 kft to about 50 kft where aerodynamic surfaces are able to control the landing maneuvers required.

Ground-Launched Vehicle Design Trades - Several ground-launched RBCC vehicle designs were evaluated. The vehicle ignition mass is shown in Figure 38 as a function of vehicle thrust-to-weight ratio at ignition ranging from 0.6 to 0.8 for transition Mach numbers of 10 and 12, and propane RBCC engine thrust-to-weight ratios ranging from 25 to 43:1. Two hydrogen RBCC cases are presented for comparison purposes, showing that a lighter vehicle (by about 30 to 40%) is possible when using hydrogen propellant in lieu of propane. The vehicle mass is seen to increase as greater ignition thrust is needed. However, the baseline vehicle design chosen for this trajectory analysis is shown at an ignition weight of 506 k lbm, an engine T/W of 43:1, and an M_T of 10.

Ground-Launched Trajectory - The baseline RCDS-GL vehicle is sized to accommodate the maximum range missions from two US hubs to cover the mission model as previously indicated in Table 4. The flight of a ground-launched vehicle is simulated on the Boeing OTIS trajectory simulation code which has the attribute to maximize range. The flyout trajectory to burnout is presented in Figure 39 for this typical vehicle design. The liftoff velocity is 450 fps at an altitude of 200 f., and an angle of attack of 17.2 deg for appropriate subsonic lift conditions. The propellant weight used on the runway is 29 klbm. The vehicle flies up an altitude-range profile at Q=2,000 psf while achieving the transition Mach number of 10 at a flight time of about 400 sec. Then, the ascent-rocket

mode takes over and the vehicle flies up to an altitude of 179 k ft which is reached at burnout after a flight time of 610.3 sec.

A typical maximum range trajectory of 7,643 nmi or 14,154 km (from Anchorage, Alaska to Perth, Australia) is presented in Figure 40. At rocket burnout the velocity achieved is 20,523 fps at a surface range of 850 nmi. The vehicle then coasts up to 190 kft before a long glide down into the denser atmosphere, achieving Mach 2 after a flight time of 4,000 sec (67 min) at an altitude of 60 kft. The vehicle's altitude descent continues, achieving Mach 1 at 20 kft, and subsonic speed at 5 kft after a flight time of 4,400 sec (73 min.). The axial rocket thrusters are available to maneuver the vehicle to the final target area while gliding to a final unpowered landing.

The vehicle flies a high dynamic pressure (Q) profile during the airbreathing mode to Mach 10, whereupon the ascent-rocket mode takes over to achieve a Mach number of about 19 at a low Q of about 200 psf, as seen in Figure 41. As the vehicle coasts up and passes over the apogee to glide back to lower altitude, the Q builds up to reach about 1,000 psf at 100 kft; as the vehicle descends to 40 kft, the Q drops to about 200 psf. Transitioning the denser atmosphere at near sonic speeds the vehicle is subjected to a higher Q (600 psf) prior to dropping off at 5,000 ft altitude to under 100 psf.

Several ground-launched trajectory cases have been evaluated for maximum vehicle temperature and heat flux experienced during the mission. The baseline heat flux is 200 BTU/ft^2-sec, which corresponds to a stagnation temperature of 3,750 deg-F, as presented in Figure 42. As seen, the heating environment constraint decreases as the maximum range achievable drops off. A range decrease of 28 percent results for a maximum heat flux of 100 BTU/ft^2-sec with a temperature of 3,100 deg-F on the nose. The thermal protection systems previously postulated for an orbital vehicle used carbon/silicon carbide (C/SiC) on the nose and leading edges of the vehicle, graphite-epoxy for the body structure and LH_2 tanks, and aluminum-lithium for the LO_2 tanks. At the higher heat flux levels of the RCDS-GL the C/SiC may have to be replaced with hafnium diboride (HfB_2) on the nose and leading edges.

The heat flux and nose stagnation temperatures for the baseline vehicle as a function of Mach number are shown, respectively, in Figures 43 and 44. The heat flux ascent profile

reaches 200 BTU/ft^2-sec near burnout and stays at this constraint during the initial glide portion of the descent trajectory from apogee. As the vehicle reenters the atmosphere the heat flux and stagnation temperature drop off; the latter follows the ascent heating temperature closely to the target landing area.

The ground-launched vehicle mission propellant mass requirements are summarized in Figure 45. This design trade is for a Los Angeles to Tokyo mission with an engine thrust-to-weight ratio of 35:1 and a maximum heat flux of 150 BTU/ft^2-sec. The baseline vehicle in this case is flown to a maximum range of 6,793 nmi (13,580 km). If the heat flux is constrained to 100 BTU/ft^2-sec then the maximum range is limited to only 5,515 nmi (10,213 km), or a loss of about 20 percent. Off-loading propellant from the baseline vehicle results in shorter ranges achievable. The baseline useable propellant mass is 373 klbm for the maximum range, which carries the vehicle 605 nmi beyond Brisbane from Los Angeles to near Perth. Off-loading propellant to 250 klbm is required to reach Tokyo from Los Angeles. A short hop to Anchorage from Los Angeles requires the loading of only 90 klb of propellant.

Air-Launched Vehicle Design Baseline - An air-launched vehicle (RCDS-AL), depicted in Figure 45, is also sized to cover the same mission model. The vehicle selected is sized in this case for an engine thrust-to-weight ratio of 35:1 and a vehicle thrust-to-weight ratio at ignition of 1.0 after aircraft separation. The total velocity used in the vehicle sizing is 23,900 fps, plus the same onboard maneuvering capability as for the ground-launched design. The gross takeoff mass of this vehicle is 390 klbm, while the useable propellant is 290 klbm. The vehicle layout, shown in Figure 46, is similar to the ground-launched vehicle previously shown in Figure 37. Depending on the propellant tank sizes the air-launched vehicle could be shorter, as the tank volumes are less for the air-launched design.

The launch platform chosen for this air-launched design is the Russian AN-225, as depicted in Figure 47. This aircraft has a payload limit of about 550 klb. The launch conditions assumed the RCDS-AL vehicle is released at an altitude of 40,000 ft and a

Mach number of 0.8 (775 fps). After separation the RBCC engines ignite and start operation in the ducted rocket modes.

Air-Launched Vehicle Design Trade - Several air-launched vehicle designs have been evaluated. The vehicle gross ignition mass is shown in Figure 48 as a function of vehicle thrust-to-weight ratios ranging from 0.6 to 1.0, for transition Mach numbers of 10 and 12, and propane Strutjet engine thrust-to-weight ratios of 30, 35 and 43:1. The vehicle mass decreases for the lower thrust levels, but the maximum range is achieved at the baseline design point with a thrust-to-vehicle weight ratio of 1.0. Again the baseline OTIS trajectory simulation is shown for an engine T/W of 35:1 and an M_T of 10, resulting in a vehicle gross weight of 390 klbm.

Air-Launched Trajectory - The baseline vehicle is sized to fly a maximum range from both US hubs. The vehicle flight is simulated on the OTIS trajectory code from aircraft launch over the Pacific Ocean to the target hub. The baseline vehicle flies up the high dynamic pressure (Q = 2,000 psf) profile to about 100 kft altitude, then the ascent-rocket mode carries the vehicle to a burnout at 181 kft altitude after a flight time of 498 sec. (8.3 min), as depicted in Figure 49. The vehicle's burnout velocity is 20,583 fps at a Mach number of about 19.5.

Figure 50 presents the altitude-range profile of the baseline vehicle flown from Anchorage to the maximum range. The baseline vehicle is able to cover Singapore and Brisbane with sufficient range to land near Perth, Australia. The flight profile is similar to the ground-launched vehicle, previously shown in Figure 40. The maximum range achieved is 7,856 nmi (14,548 km), and the vehicle reaches an apogee altitude of about 200 kft prior to the long glide back to the lower atmosphere. The dynamic pressure buildup is also similar to the ground-launched case, and reentry at Mach 1 (20 kft altitude) is achieved after 4,200 sec (70 min) flight time. Another 100 sec is taken to reach the target area flying subsonically. The onboard reaction-control system (RCS) is used to stabilize the vehicle during the glide phase from apogee. The onboard maneuvering rocket system (OMS) of 1,000 fps velocity capability allows the vehicle to fly to alternate bases and/or readjust the range, as needed, during the flight.

The air-launched vehicle mission propellant mass requirements are summarized in Figure 51. This design trade example is for flights from the Anchorage base to shorter ranges. For flights to Brisbane the propellant loading needs to be only 80 percent of the nominal 290 klbm propellant. For flights to Tokyo the loading reduces to 39 percent of maximum. Off-loading propellant from the baseline vehicle results in the shorter ranges achievable.

7.0 Summary and Conclusions

Two propane fueled rapid cargo delivering systems vehicles have been presented capable to operate at hypersonic speeds between hubs around the Pacific rim countries. With flight times between hubs below 90 min, and the ability for either ground or airlaunch, an attractive new transportation system can be envisioned. This system is suitable for performing its missions in an environmentally acceptable fashion relative to the generation of noise and air pollution. Noise is mitigated by subsonic shuttle service of the cargo to and from the hubs, and air launch of the hypersonic vehicle to an noise insensitive launch site. Air pollution is minimized through the use of relatively clean burning propane propellant. These vehicles may have the potential to operate eventually in an airline type fashion with long mean times between overhaul, bringing operating cost down levels where new markets will open up. The key to this potential is the abandonment of the power density operation of all-rocket propulsion in favor of a more benign rocket based combined cycle propulsion concept.

Hydrogen And Hydrocarbon Strutjet Engines - These engines, particular the hydrogen fueled one, have made considerable progress, and test data established to date verify their fundamental feasibility and support earlier performance predictions. While the current NASA Advanced Reusable Technology (ART) Program as well as Aerojet sponsored test activities will provide additional data during 1998 and early 1999, no further design or test activities are currently planned for storable hydrocarbon RBCC engines.

Strujet Technology Maturity - Although significant achievements have been made towards a Technology readiness Level of 6, demonstration in a relevant environment, most of the effort to date is focused on flowpath development and performance assessment. Future work must be done on engine structure, thermal management, and propellant feed system. Ground tests of flight type engines are mandatory before committing these advanced engines to in-flight, captive carry or self-powered, evaluation.

Rapid Cargo Delivery System - Advanced RBCC Strutjet vehicle designs using LO_2/LC_2H_8 propellants have the potential to offer robust vehicles capable to perform rapid cargo delivery missions to various points around the Pacific rim to and from US hubs. Even though a LO_2/LH_2 design would have a lower gross weight, the use of propane in lieu of hydrogen allows easier handling and storage of propellants. Air-launched vehicles flying from an AN-225 aircraft may be safer with propane onboard than with a hydrogen vehicle. Vehicles transporting a 5,000 lb cargo may offer delivery of the payload in flight times of about 1 hour, depending on the mission base destination. Ground vehicles weighing about 480 klbm and air vehicles weighing about 390 klbm could be designed to reach the major city ports around the Pacific rim, and possibly to Europe when flying over the North Pole.

Advanced thermal protection system (TPS) materials may have to be developed to handle the heat flux and leading edge temperature environments experienced in flying ranges out to 14,000 km. Maximum range achievable is decreased for lower heating design constraints.

The vehicle/engine designs presented establish first order feasibility of rapid cargo delivery systems. If future economic studies can support the need and profitability of such system, more in depth engine and vehicle designs are required and recommended.

7.0 References

1. William Scott, "....." Aviation Week, June 15, 1998
2. Penn J.A. and Lindley C.A., The Aerospace Corporation, 2350 E. El Segundo Bl., El Segundo, California, 90245-4691, "Requirements And Approach For A Space Tourism Launch System"

3. Bulman, M.J. and Siebenhaar, A., Aerojet Propulsion Division, Sacramento, California, " Rocket Based Combined Cycle Propulsion For Space Launch", 46th International Astronautical Congress, 1995 / Oslo, Norway, IAF-95-S.5.02
4. Siebenhaar, A., GenCorp Aerojet, Sacramento, California, and D.K. Bonnar, The Boeing Phantom Works, Huntington Beach, California, "Strutjet Engine Paves Road To Low Cost Space Access", 48th International Astronautical Congress, 1997/ Turin, Italy, IAF-97-S.5.05
5. US Patent No. 5,220,787 " Scramjet Injector", issued to Aerojet June 22, 1993

Table 1:

Parameter	Design	Nominal Operation
Mixture Ratio	1.6	1.4
Chamber Pressure (psia)	2,500	1600–2000
Thrust (lbf)	1,000	600–700
Expansion Ratio	5.1 and 11.1	5.1 and 11.1

Table 2:

Chamber Pressure (psia)	Mixture Ratio	Test Duration (sec)
100 – 1800	4.76 – 7.0	1 – 5

Table 3:

Top Level Technology Item	Sub Tier Technology Item	Degree of Technology Maturity		
		Low	Medium	High
Flowpath Integration	Design Point Selection		x	
	Balanced Performance Along Flowpath		x	
Fuel Injection	Penetration, Mixing, Vaporization		x	
	Stable Combustion		x	
	Controlled Heat release		x	
Light Weight Structure	High Temperature Materials			x
	Radiation Cooled Structures	x		
	Regeneratively Cooled Structures	x		
	Endothermic Fuel Reactions		x	
	Closed Loop Cooling	x		
Strut Rockets	High Thrust-To-Mass			x
	Long Life		x	
Turbo Pumps	Low Weight	x		
	Long Life Bearings		x	
	Low Temperature Turbines		x	
	Multi Mode Operation	x		
Engine Controls	For All Flight Modes	x		
Testing	Ground Test Subscale		x	
	Ground test Full Scale	x		
	Captive Flight Of Engine Module	x		
	Self-Powered Flight Of Flight Type Engine	x		

TABLE 1/4

Cargo Mission Ranges From Anchorage and Los Angeles

City	Main U.S. Bases		Singapore	Hong Kong	Manila	Tokyo	Brisbane	Kirma
	Los Angeles	Anchorage						
Los Angeles	0	3,768	14,111	11,646	11,742	8,816	11,461	8,863
Anchorage	3,768	0	10,797	8,335	8,538	5,591	11,466	6,078
Singapore	14,111	10,797	0	2,467	2,336	5,301	6,866	9,738
Hong Kong	11,646	8,335	2,467	0	765	2,952	7,713	8,203
Manila	11,742	8,538	2,336	765	0	2,977	6,953	8,930
Tokyo	8,816	5,591	5,301	2,952	2,977	0	8,025	7,728
Brisbane	11,461	11,466	6,866	7,713	6,953	8,025	0	15,704
Kirma	8,863	6,078	9,738	8,203	8,930	7,728	15,704	0

Note: Range in Kilometers

BOEING

02760VEU8.2

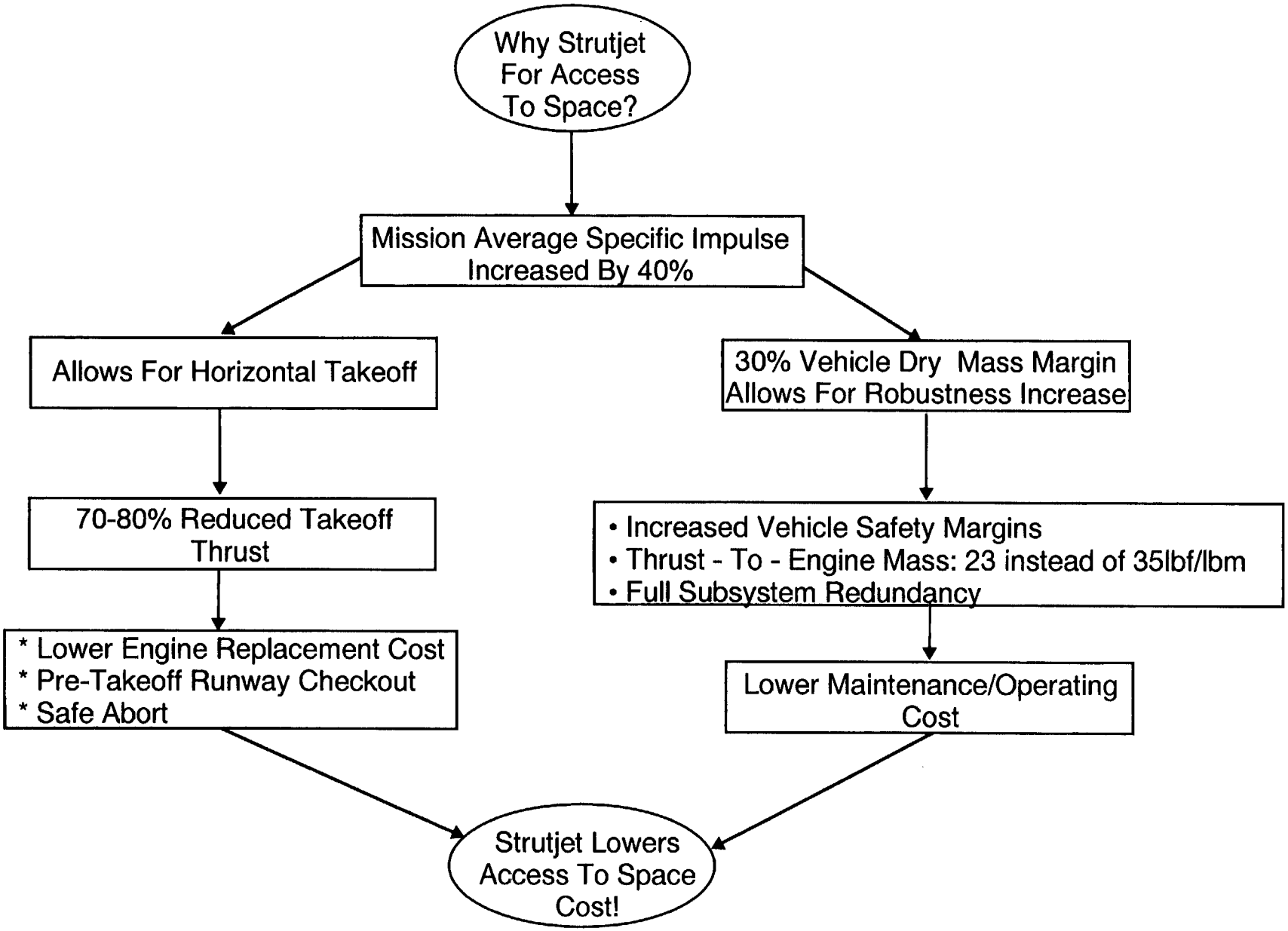
Why Strutjet For Access To Space?
Mission Average Specific Impulse Increased By 40%
Allows For Horizontal Takeoff
30% Vehicle Dry Mass Margin Allows For Robustness Increase
70-80% Reduced Takeoff Thrust
• Increased Vehicle Safety Margins
• Thrust - To - Engine Mass: 23 instead of 35lbf/lbm
• Full Subsystem Redundancy
* Lower Engine Replacement Cost
* Pre-Takeoff Runway Checkout
* Safe Abort
Lower Maintenance/Operating Cost
Strutjet Lowers Access To Space Cost!

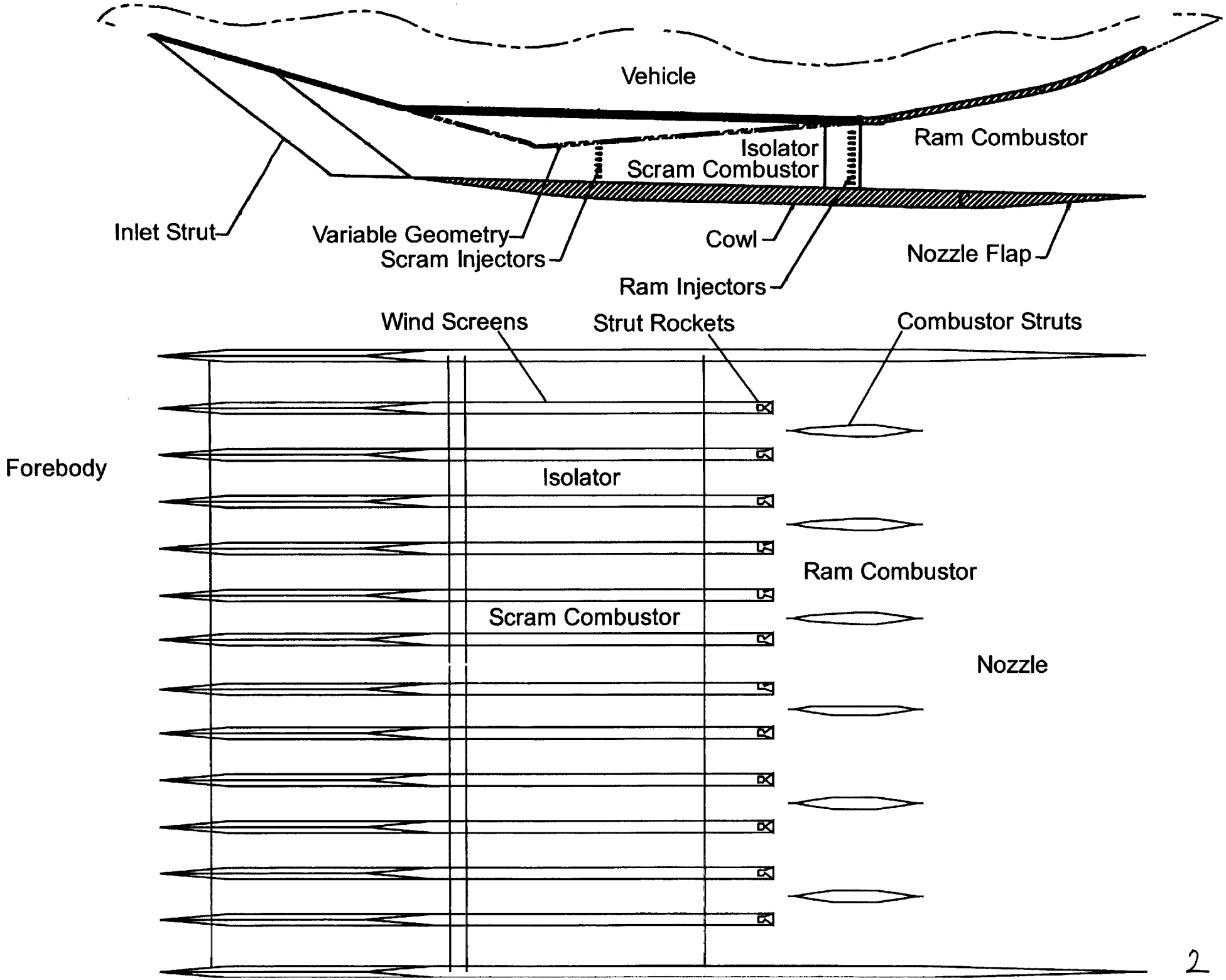
Vehicle
Isolator
Scram Combustor
Ram Combustor
Inlet Strut
Variable Geometry
Scram Injectors
Cowl
Nozzle Flap
Ram Injectors
Wind Screens
Strut Rockets
Combustor Struts
Forebody
Isolator
Ram Combustor
Scram Combustor
Nozzle

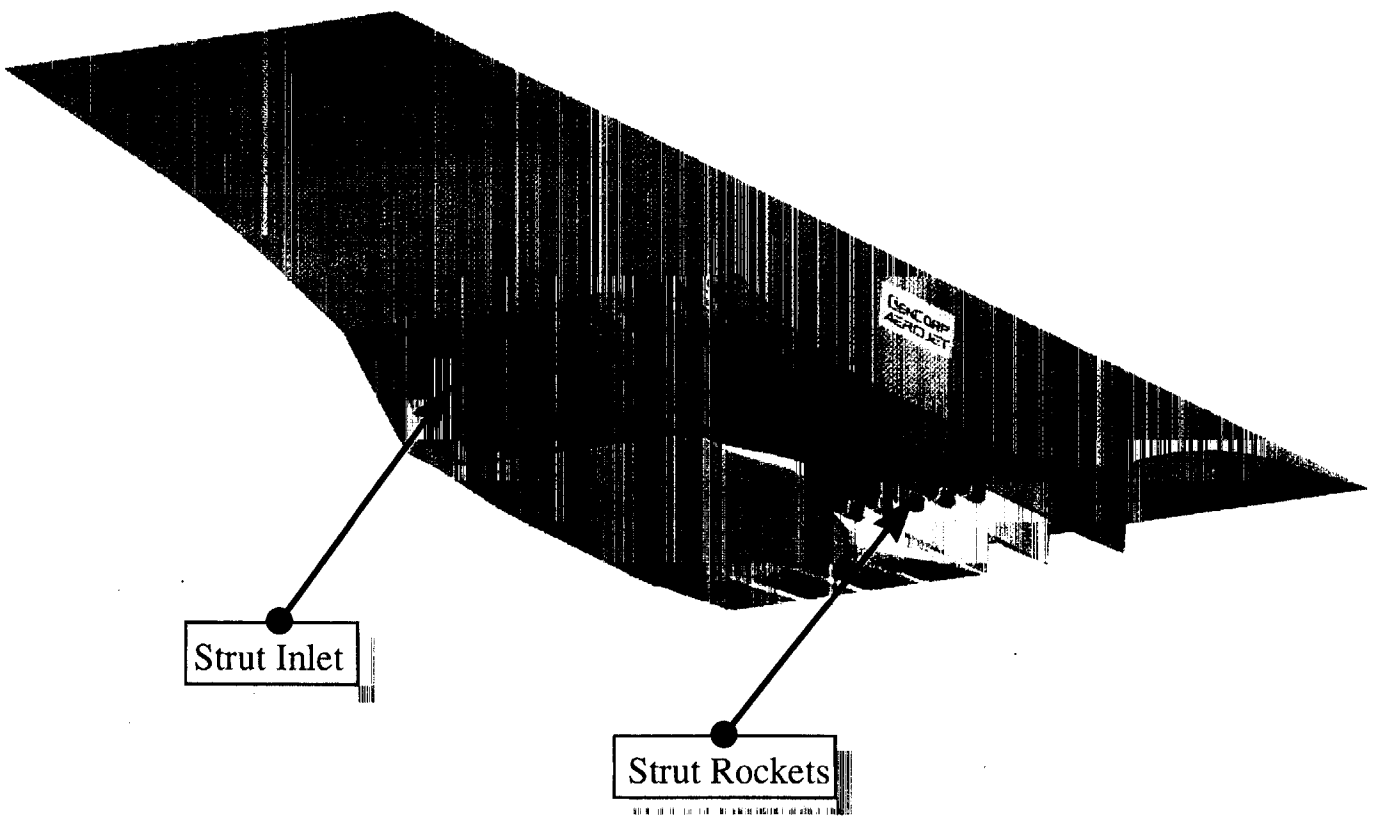
Strut Inlet
Strut Rockets

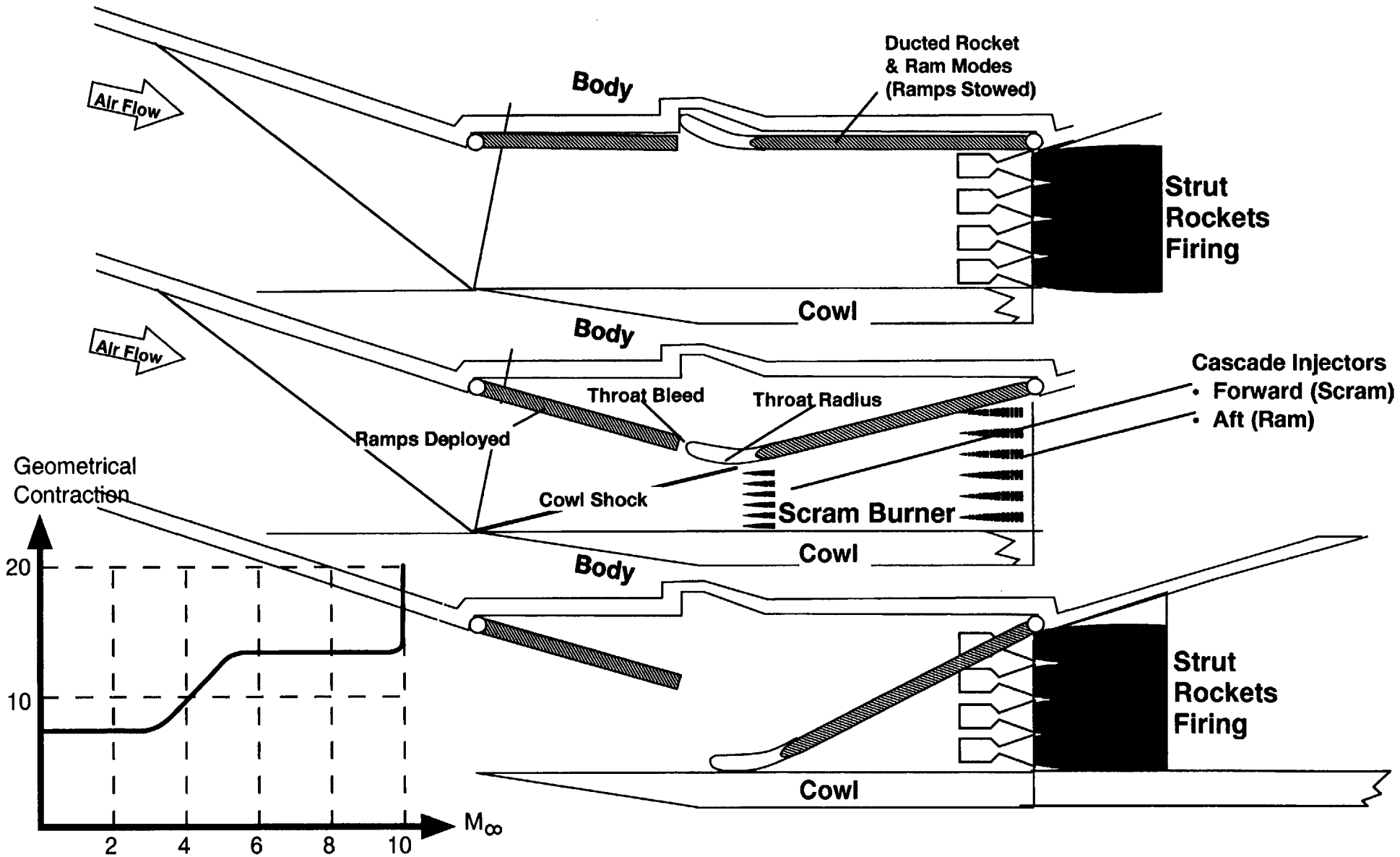
Ducted Rocket
& Ram Modes
(Ramps Stowed)
Body
Air Flow
Strut
Rockets
Firing
Cowl
Body
Air Flow
Cascade Injectors
• Forward (Scram)
• Aft (Ram)
Throat Bleed
Throat Radius
Ramps Deployed
Cowl Shock
Scram Burner
Cowl
Body
Strut
Rockets
Firing
Cowl
Geometrical
Contraction
20
10
2
4
6
8
10
M∞

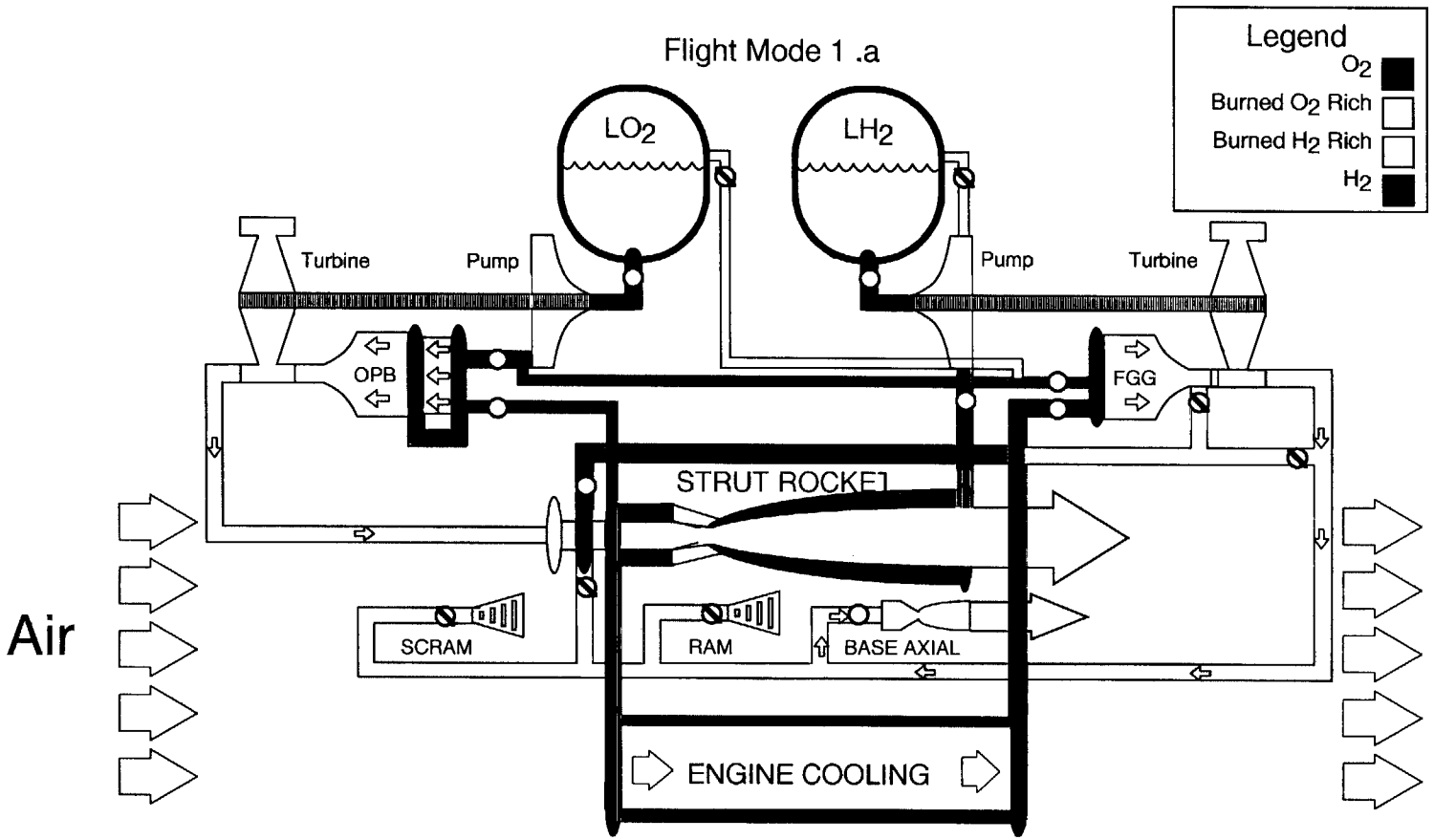

Mode	Cycle O_2	Cycle H_2
1. a. Ducted Rocket	PB	GG
b. Ducted Rocket	PB	GG
c. Ducted Rocket	PB	Exp
2. Ramjet	Off	Exp
3. Scramjet	Off	Exp
4. Scramjet/Rocket	PB	Exp
5. Unducted Rocket	PB	Exp

Rocket Flow

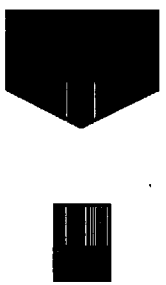

Ramjet Fuel Flow

Base Aft Fwd

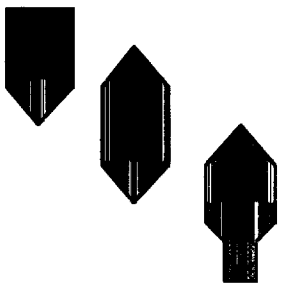

Geometry

Inlet Nozzle

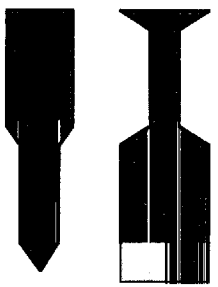

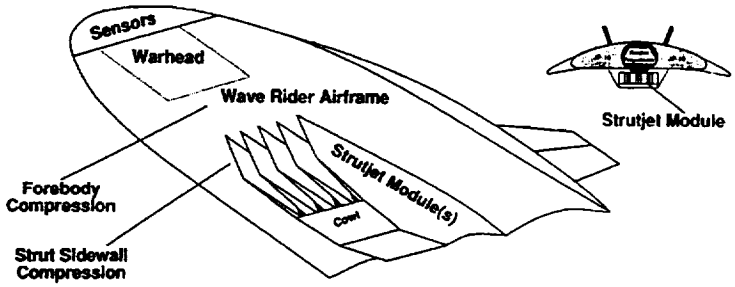
Sensors
Warhead
Wave Rider Airframe
Strutjet Module
Strutjet Module(s)
Cowl
Forebody Compression
Strut Sidewall Compression

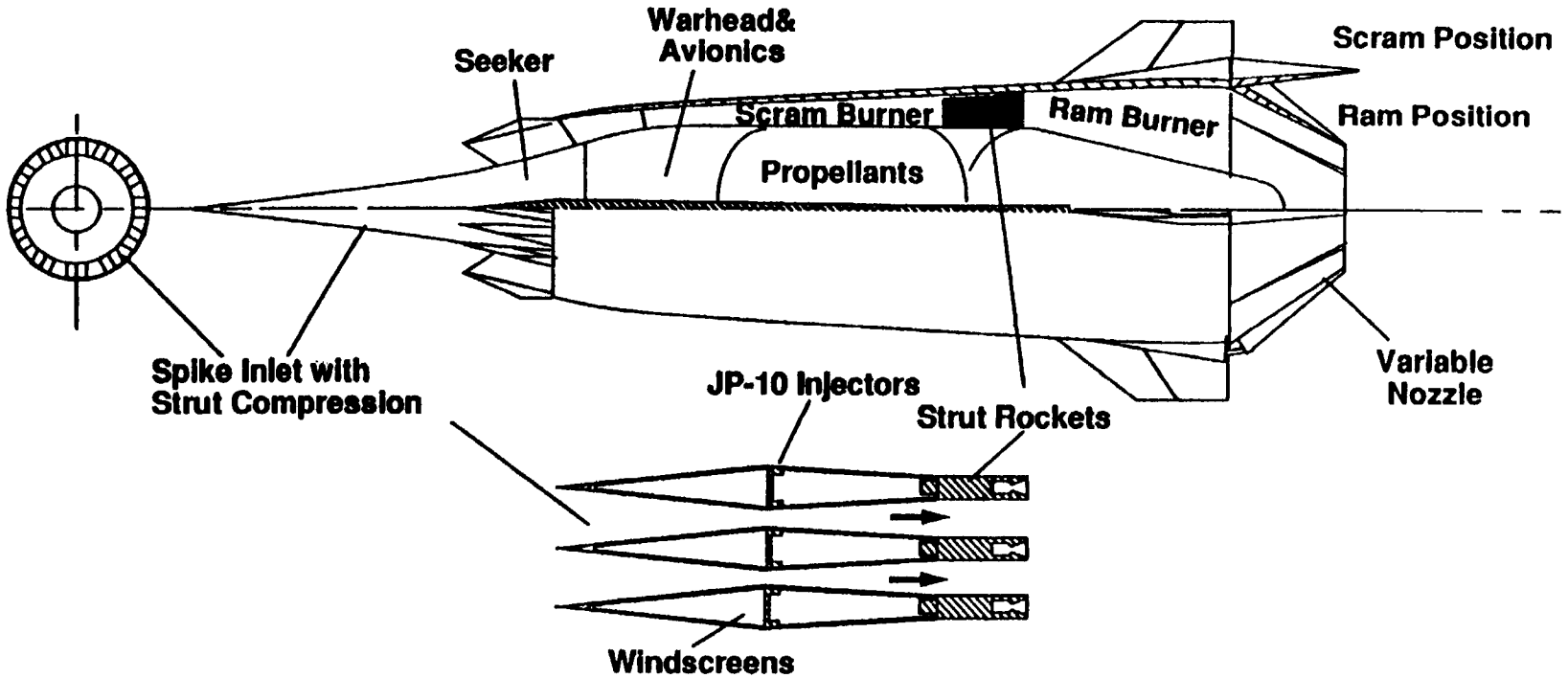
Warhead&
Avionics
Seeker
Scram Position
Scram Burner
Ram Burner
Ram Position
Propellants
Spike Inlet with
Strut Compression
JP-10 Injectors
Strut Rockets
Variable
Nozzle
Windscreens

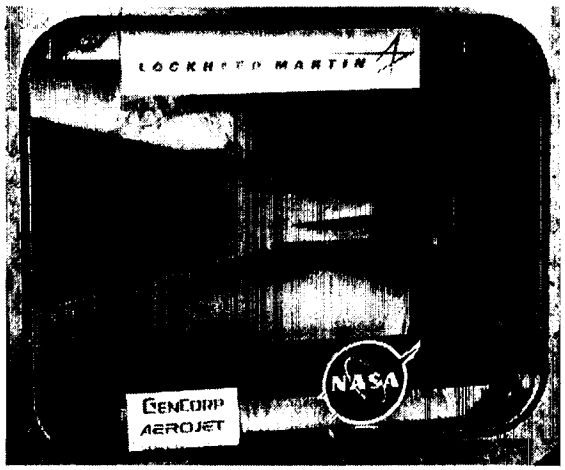
LOCKHEED MARTIN
NASA
GENCORP
AEROJET

b

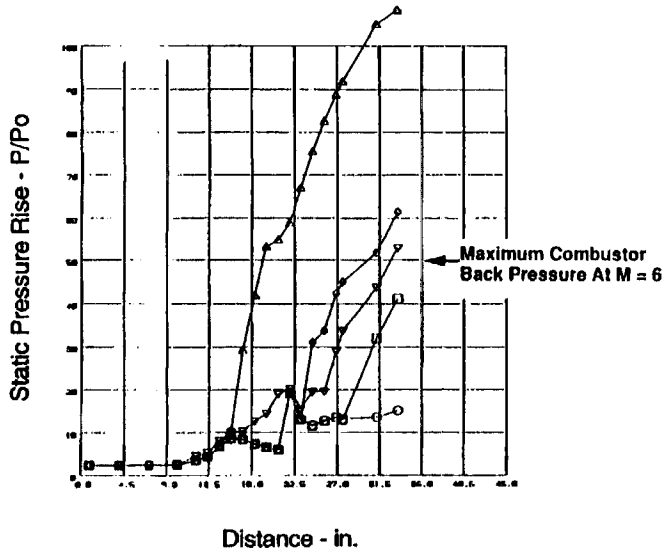
Static Pressure Rise - P/Po
Maximum Combustor
Back Pressure At M = 6
Distance - in.

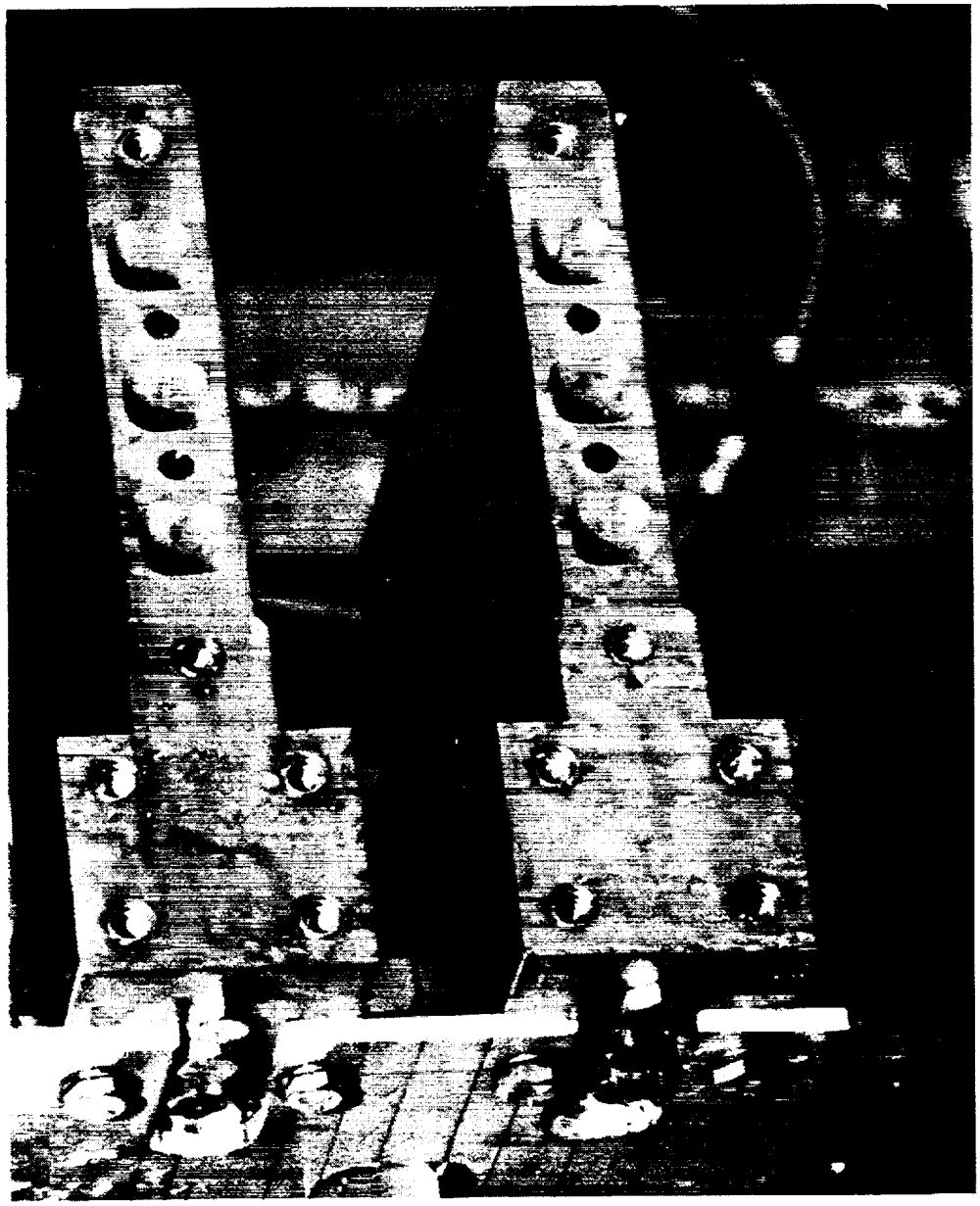

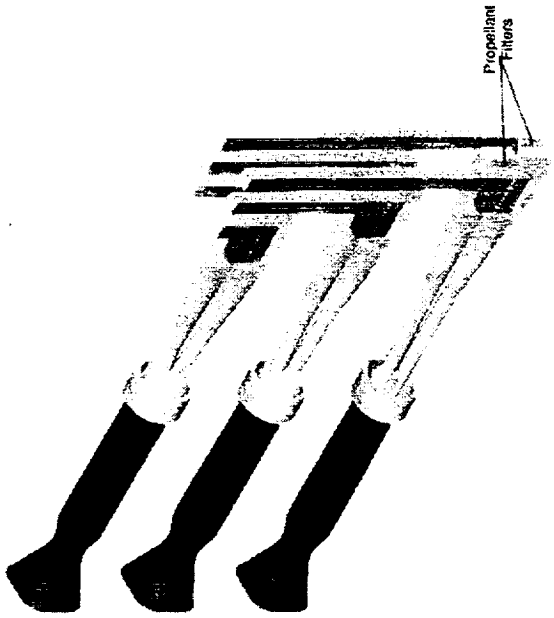
Propellant
Filters

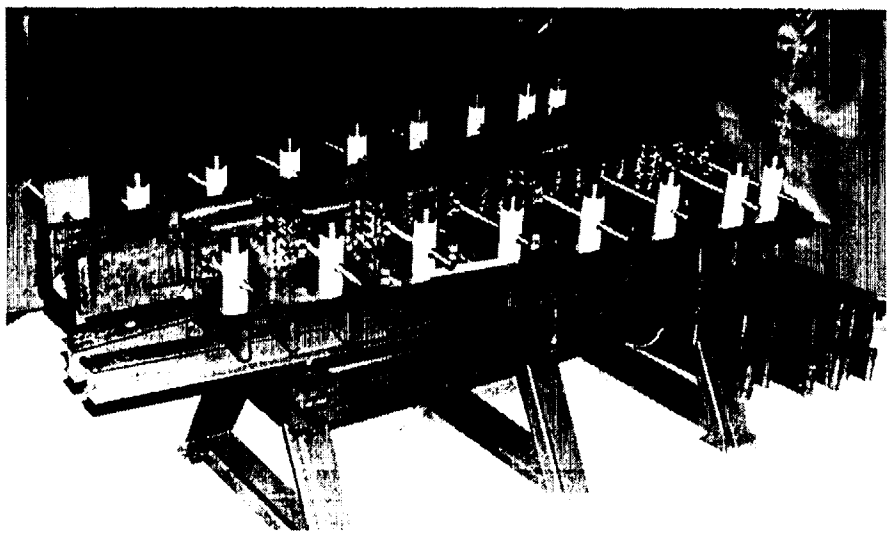

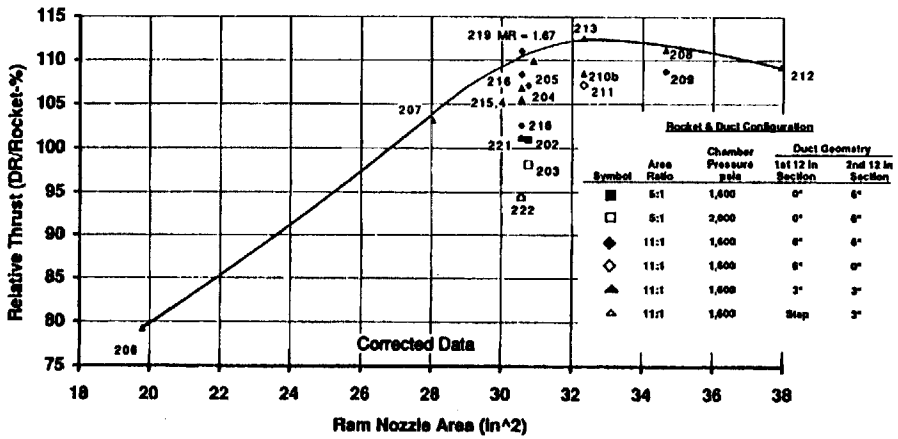
Relative Thrust (DR/Rocket-%)
Ram Nozzle Area (In^2)
115
110
105
100
95
90
85
80
75
18
20
22
24
26
28
30
32
34
36
38
219 MR = 1.67
213
208
209
212
210b
211
216
205
204
215.4
207
218
221
202
203
222
208
Corrected Data
Rocket & Duct Configuration
Symbol
Area Ratio
Chamber Pressure psia
Duct Geometry
1st 12 in Section
2nd 12 in Section
5:1
1,600
0"
6"
5:1
2,800
0"
6"
11:1
1,600
6"
6"
11:1
1,600
6"
6"
11:1
1,600
3"
3"
11:1
1,600
Step
3"

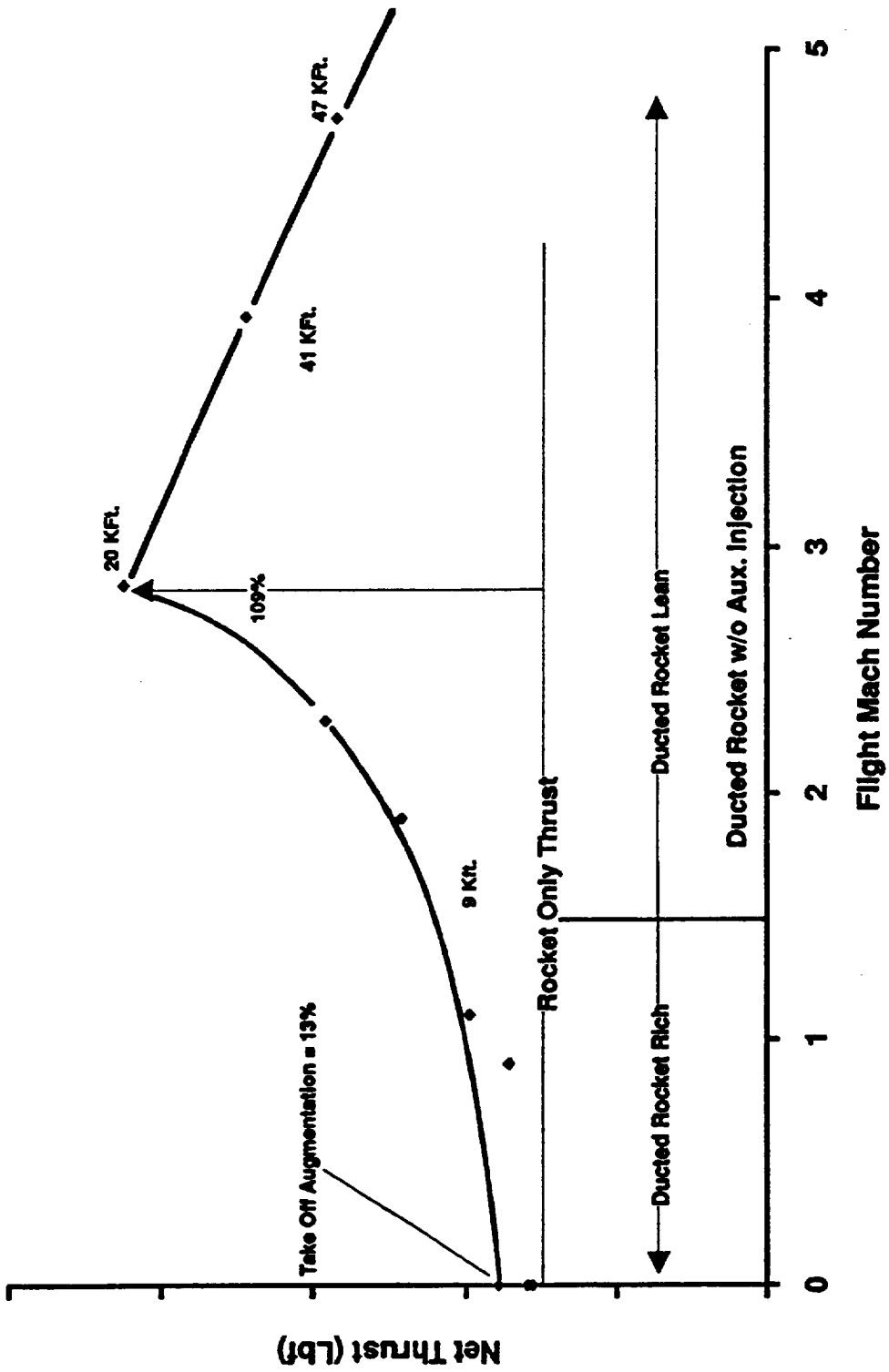
Net Thrust (Lbf)
Flight Mach Number
0
1
2
3
4
5
Take Off Augmentation = 13%
9 Klt.
20 KFt.
41 KFt.
47 KFt.
109%
Rocket Only Thrust
Ducted Rocket Rich
Ducted Rocket Lean
Ducted Rocket w/o Aux. Injection

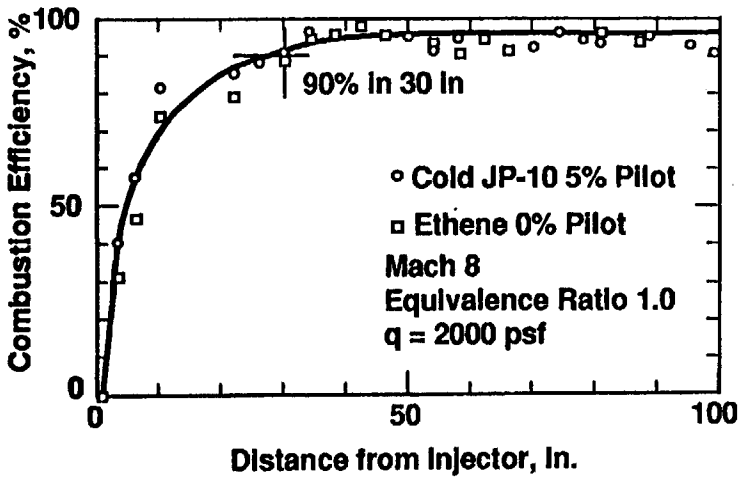
Combustion Efficiency, %
100
50
0
0
50
100
Distance from Injector, In.
90% In 30 In
Cold JP-10 5% Pilot
Ethene 0% Pilot
Mach 8
Equivalence Ratio 1.0
q = 2000 psf

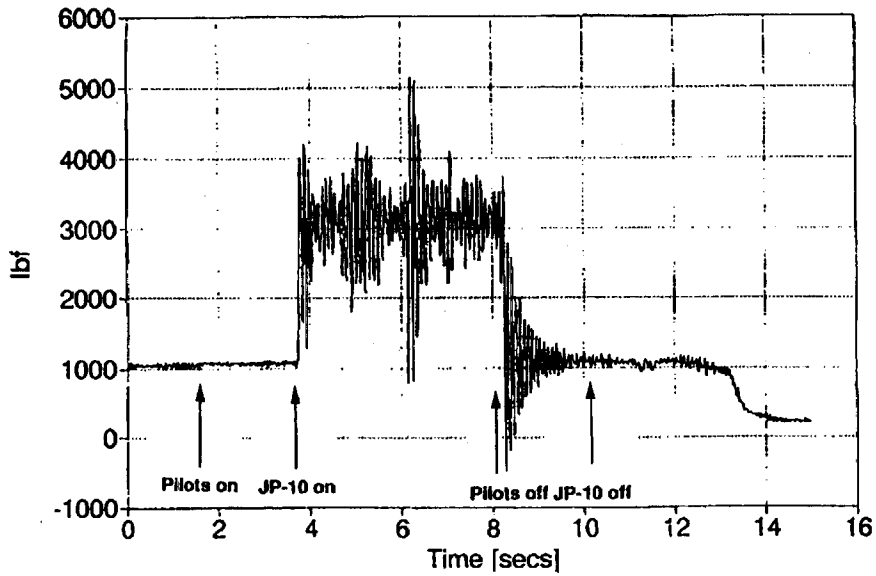
6000
5000
4000
3000
2000
1000
0
-1000
lbf
0
2
4
6
8
10
12
14
16
Time [secs]
Pilots on
JP-10 on
Pilots off JP-10 off

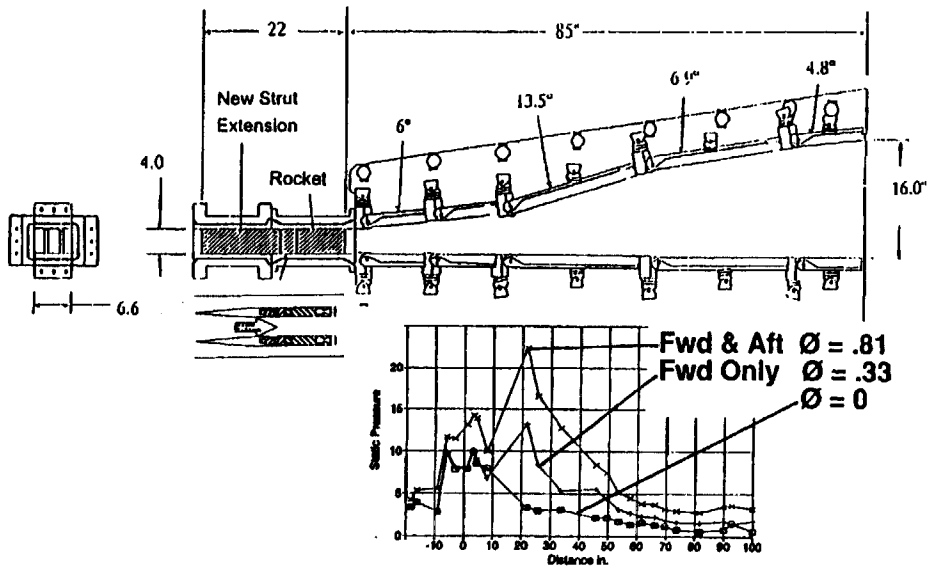
22
85"
New Strut
Extension
Rocket
4.0
6"
13.5"
6.5"
4.8"
16.0"
6.6
Fwd & Aft Ø = .81
Fwd Only Ø = .33
Ø = 0
Static Pressure
Distance in.

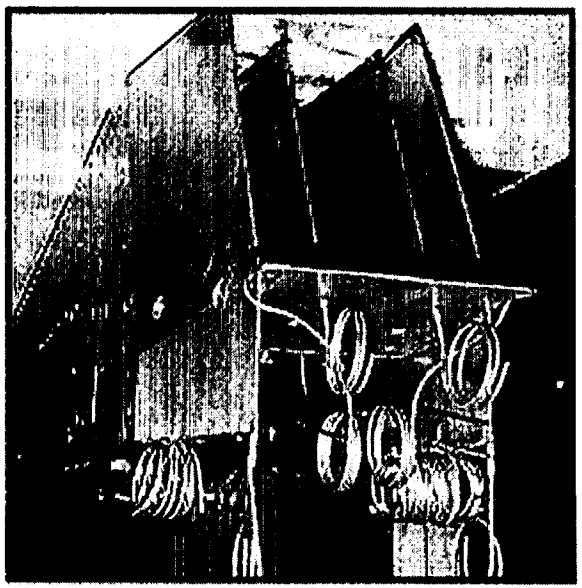

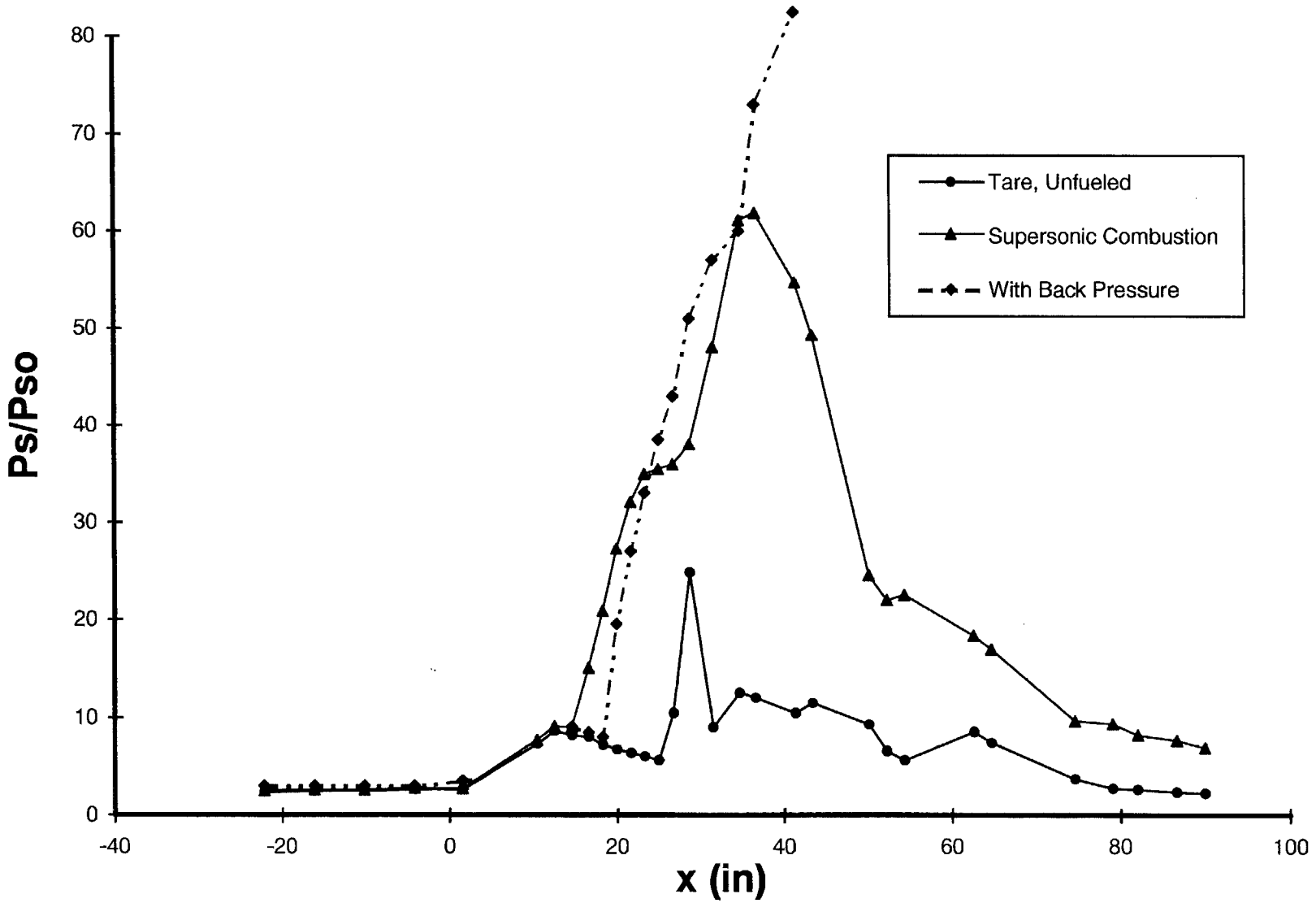
Ps/Pso
80
70
60
50
40
30
20
10
0
-40
-20
0
20
40
60
80
100
x (in)
Tare, Unfueled
Supersonic Combustion
With Back Pressure

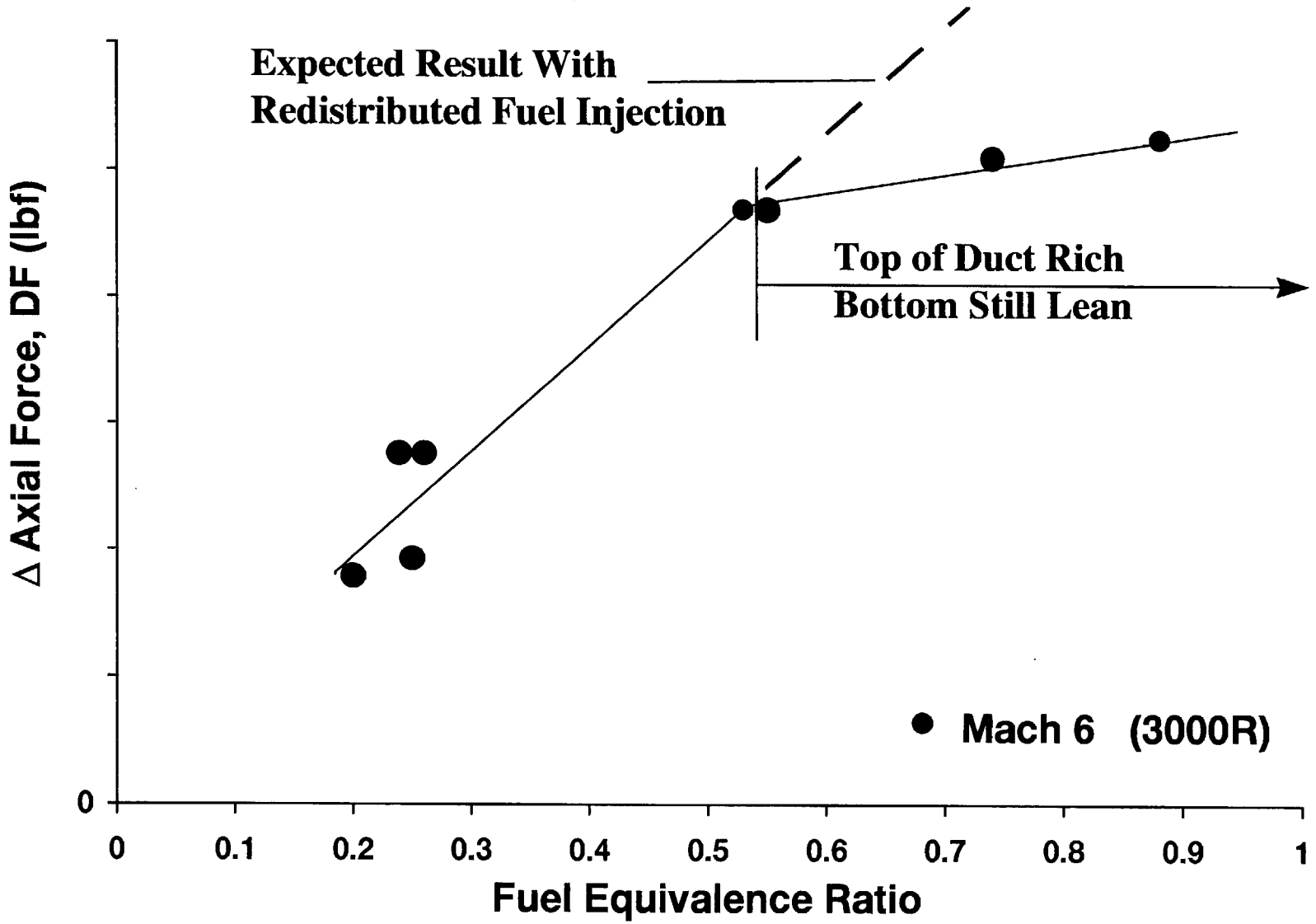
Expected Result With
Redistributed Fuel Injection
Top of Duct Rich
Bottom Still Lean
Mach 6 (3000R)
Δ Axial Force, DF (lbf)
0
0
0.1
0.2
0.3
0.4
0.5
0.6
0.7
0.8
0.9
1
Fuel Equivalence Ratio

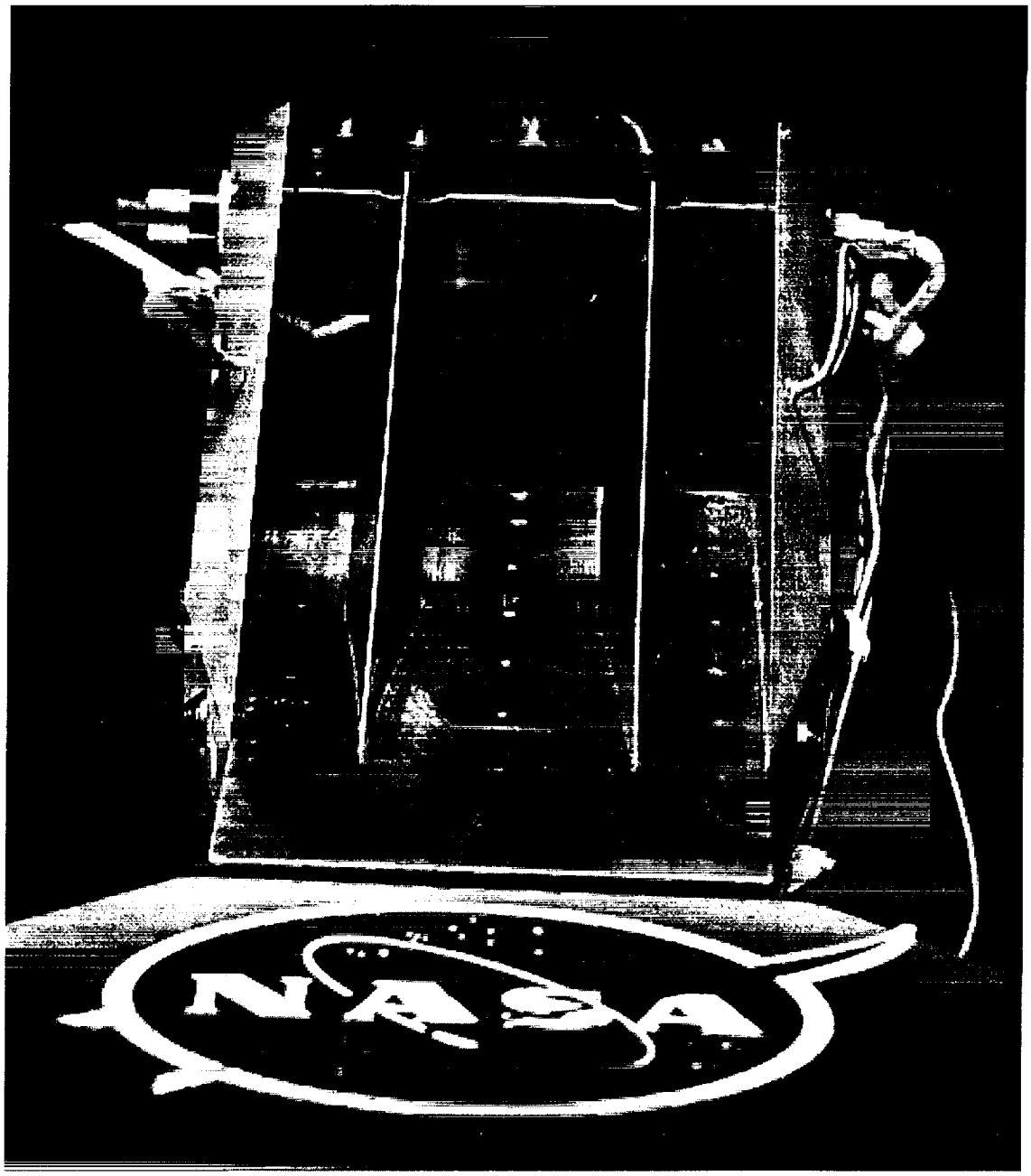
NASA

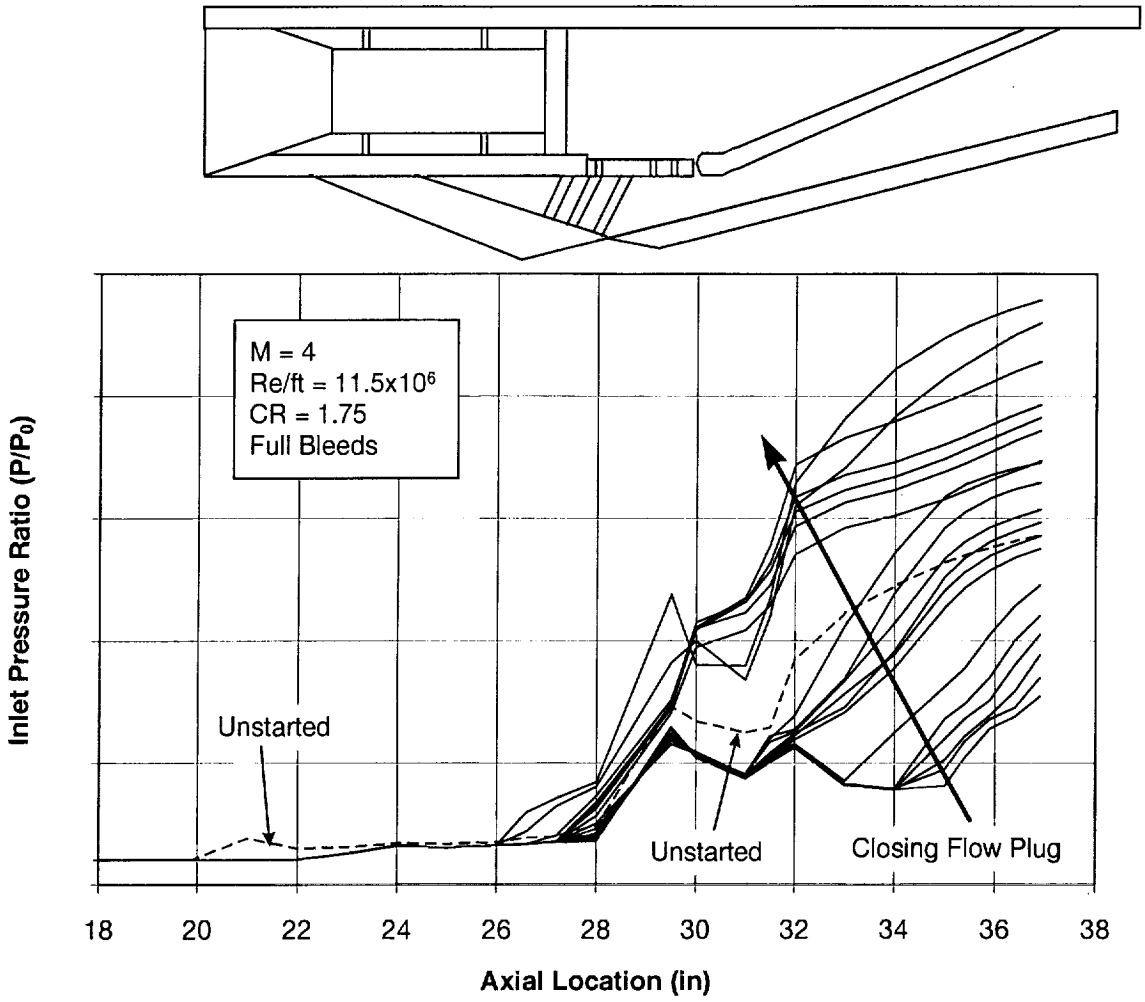
M = 4
Re/ft = 11.5x10⁶
CR = 1.75
Full Bleeds
Unstarted
Unstarted
Closing Flow Plug
Inlet Pressure Ratio (P/P₀)
18
20
22
24
26
28
30
32
34
36
38
Axial Location (in)

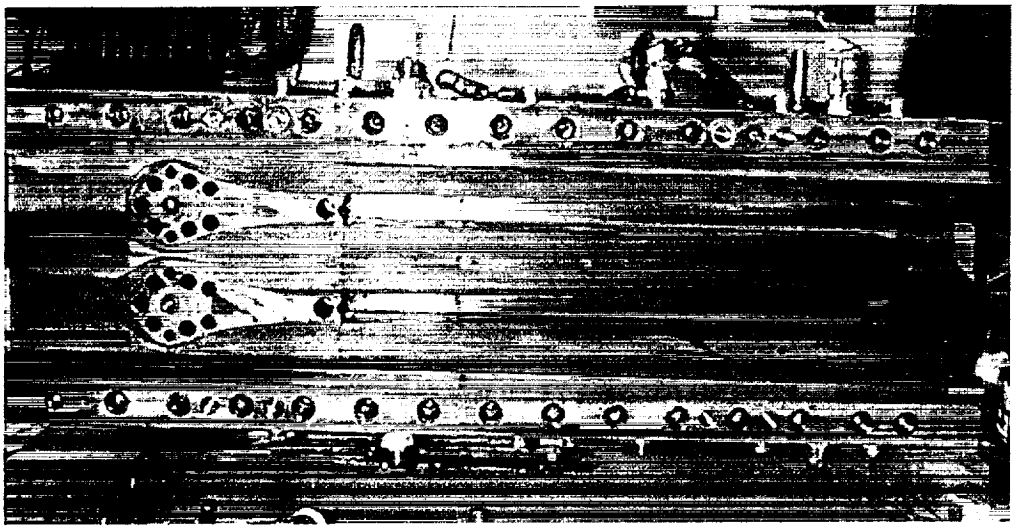

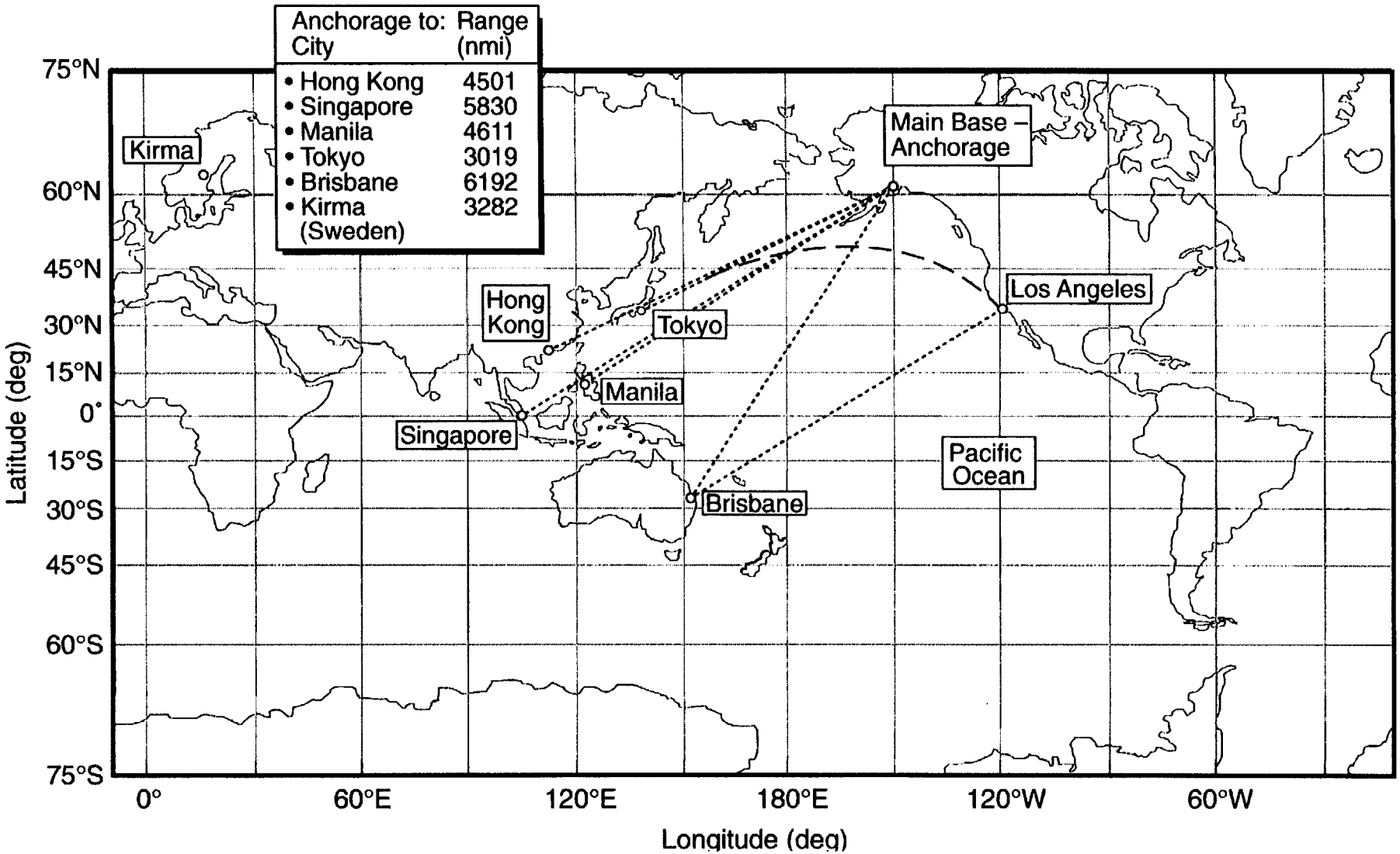
Anchorage to: City
Range (nmi)
• Hong Kong 4501
• Singapore 5830
• Manila 4611
• Tokyo 3019
• Brisbane 6192
• Kirma (Sweden) 3282
Kirma
Main Base – Anchorage
Los Angeles
Hong Kong
Tokyo
Manila
Singapore
Pacific Ocean
Brisbane
75°N
60°N
45°N
30°N
15°N
0°
15°S
30°S
45°S
60°S
75°S
Latitude (deg)
0°
60°E
120°E
180°E
120°W
60°W
Longitude (deg)

RBCC Engine Model Shows High I_{SP} During Air Breather Modes

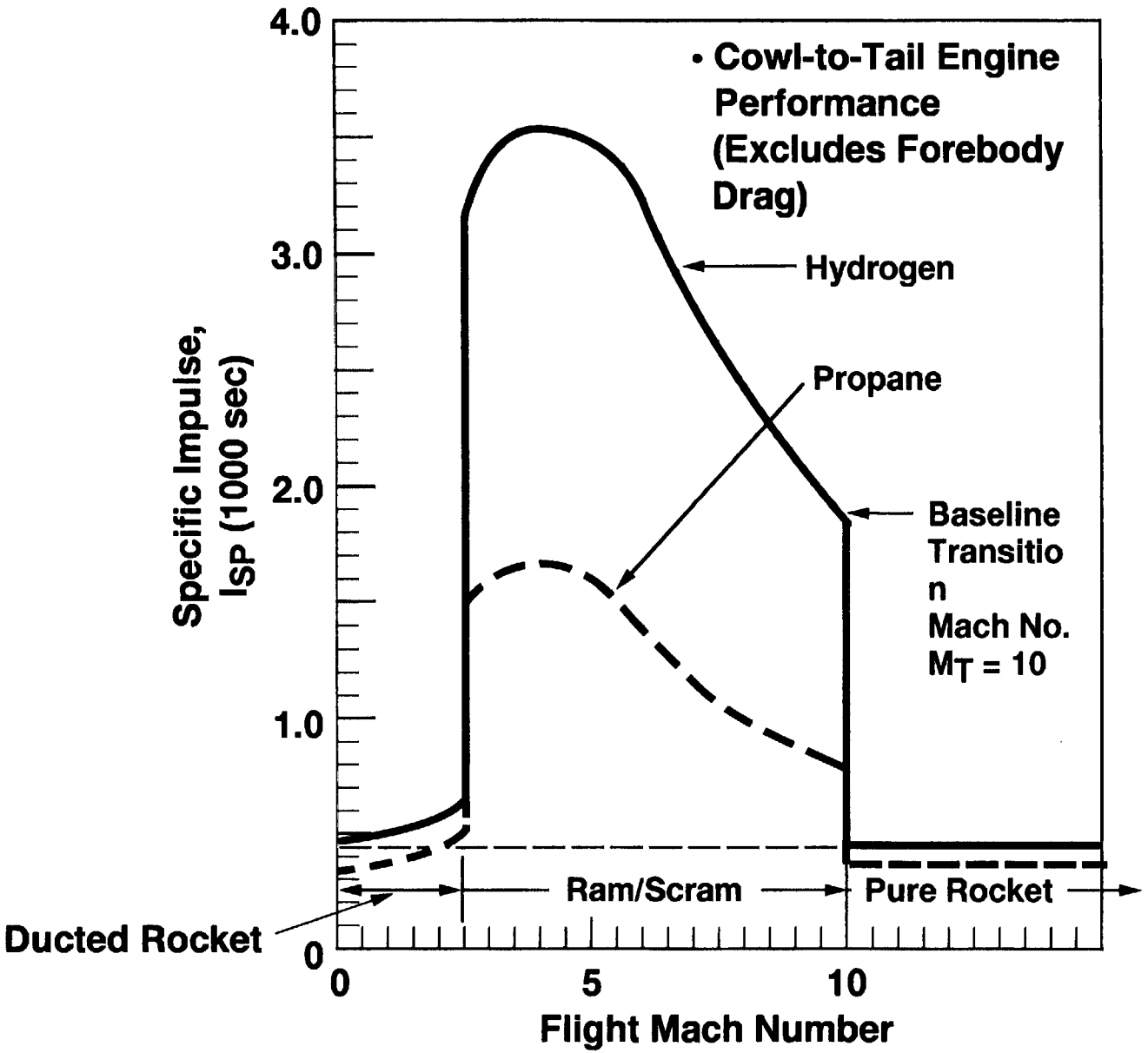

BOEING
02159VEU8

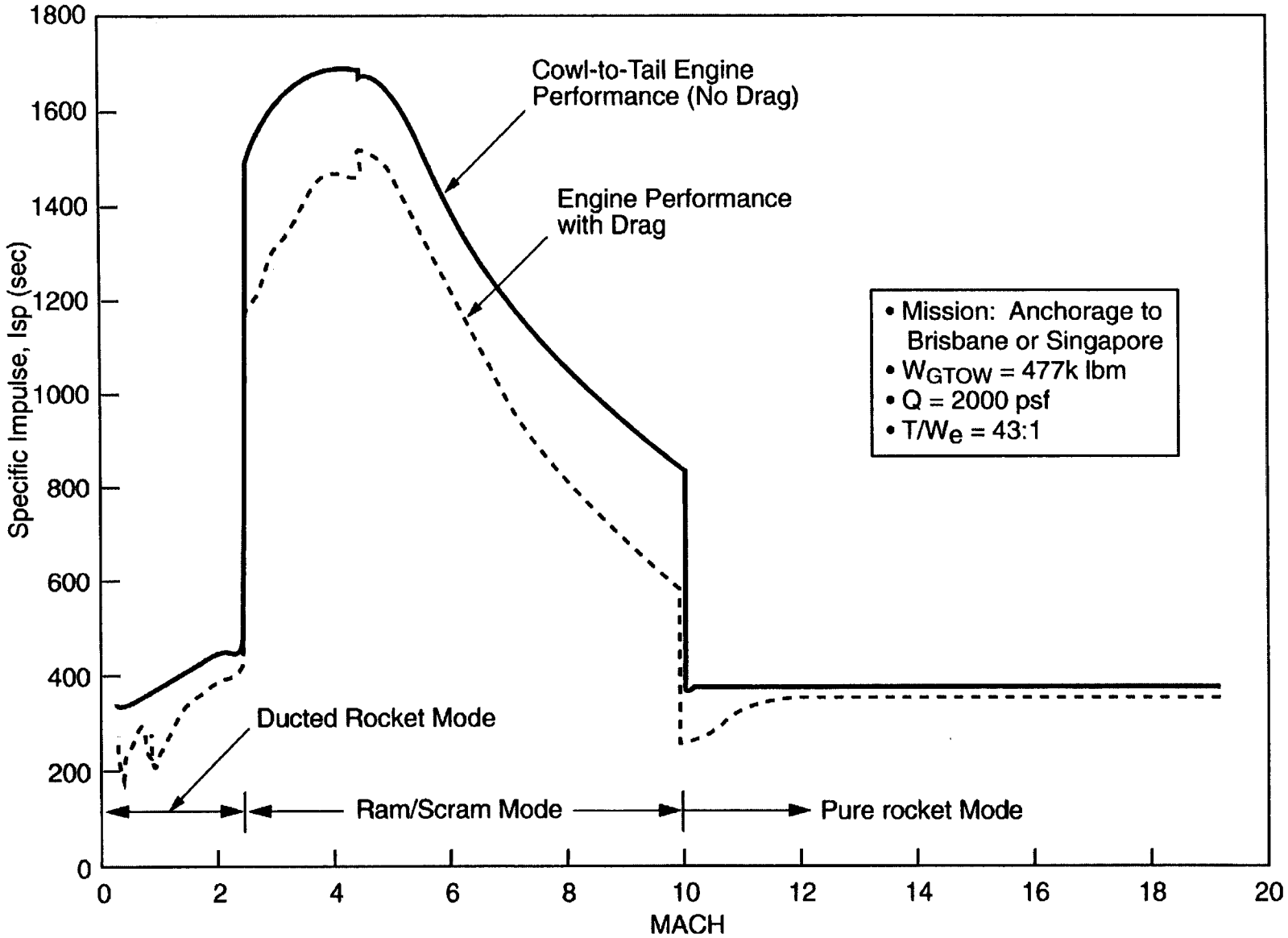
Specific Impulse, Isp (sec)
1800
1600
1400
1200
1000
800
600
400
200
0
0
2
4
6
8
10
12
14
16
18
20
MACH
Cowl-to-Tail Engine Performance (No Drag)
Engine Performance with Drag
• Mission: Anchorage to Brisbane or Singapore
• W_{GTOW} = 477k lbm
• Q = 2000 psf
• T/W_e = 43:1
Ducted Rocket Mode
Ram/Scram Mode
Pure rocket Mode

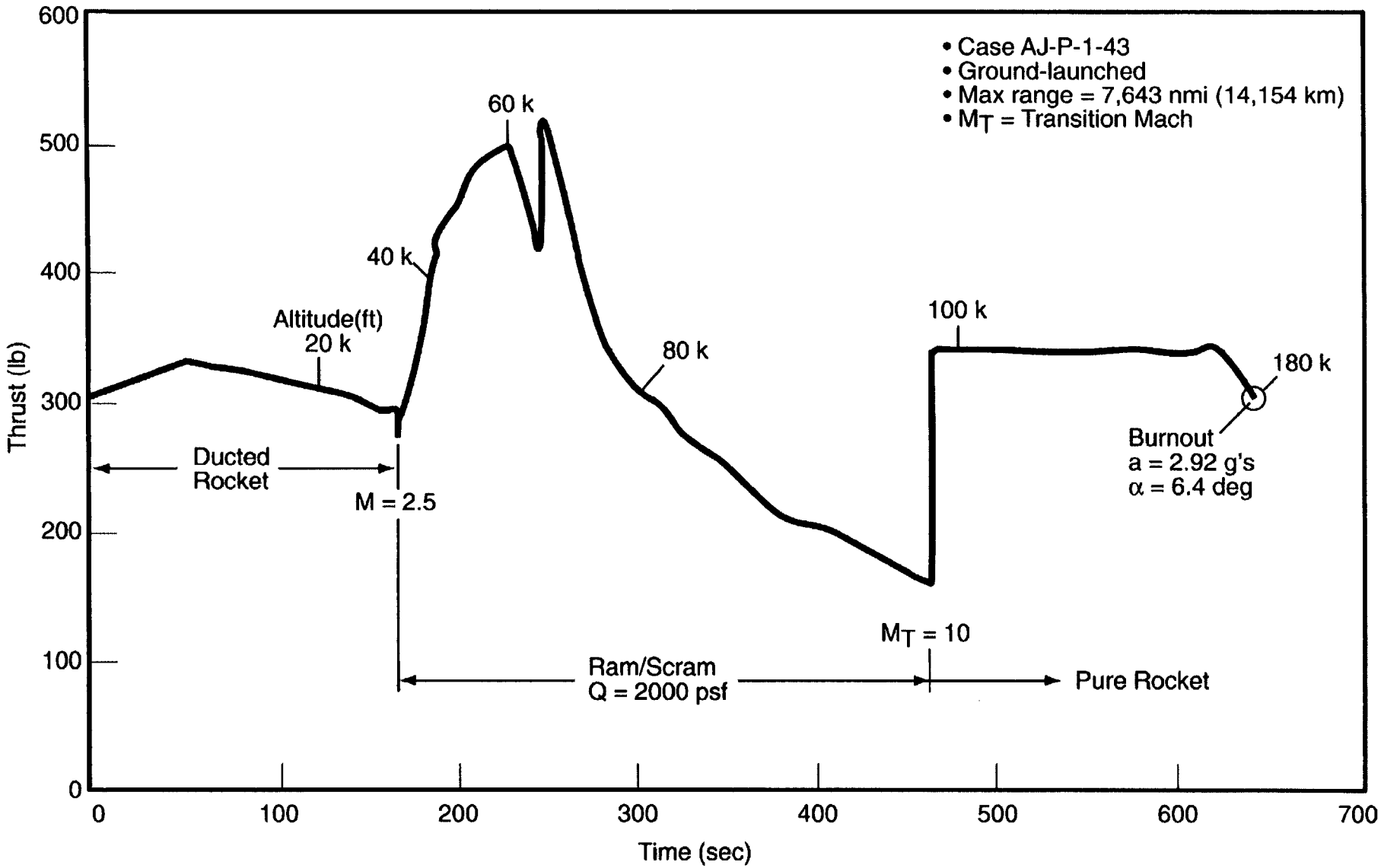
• Case AJ-P-1-43
• Ground-launched
• Max range = 7,643 nmi (14,154 km)
• M_T = Transition Mach
Thrust (lb)
Time (sec)
600
500
400
300
200
100
0
0
100
200
300
400
500
600
700
60 k
40 k
Altitude(ft)
20 k
80 k
100 k
180 k
Burnout
a = 2.92 g's
α = 6.4 deg
Ducted
Rocket
M = 2.5
M_T = 10
Ram/Scram
Q = 2000 psf
Pure Rocket

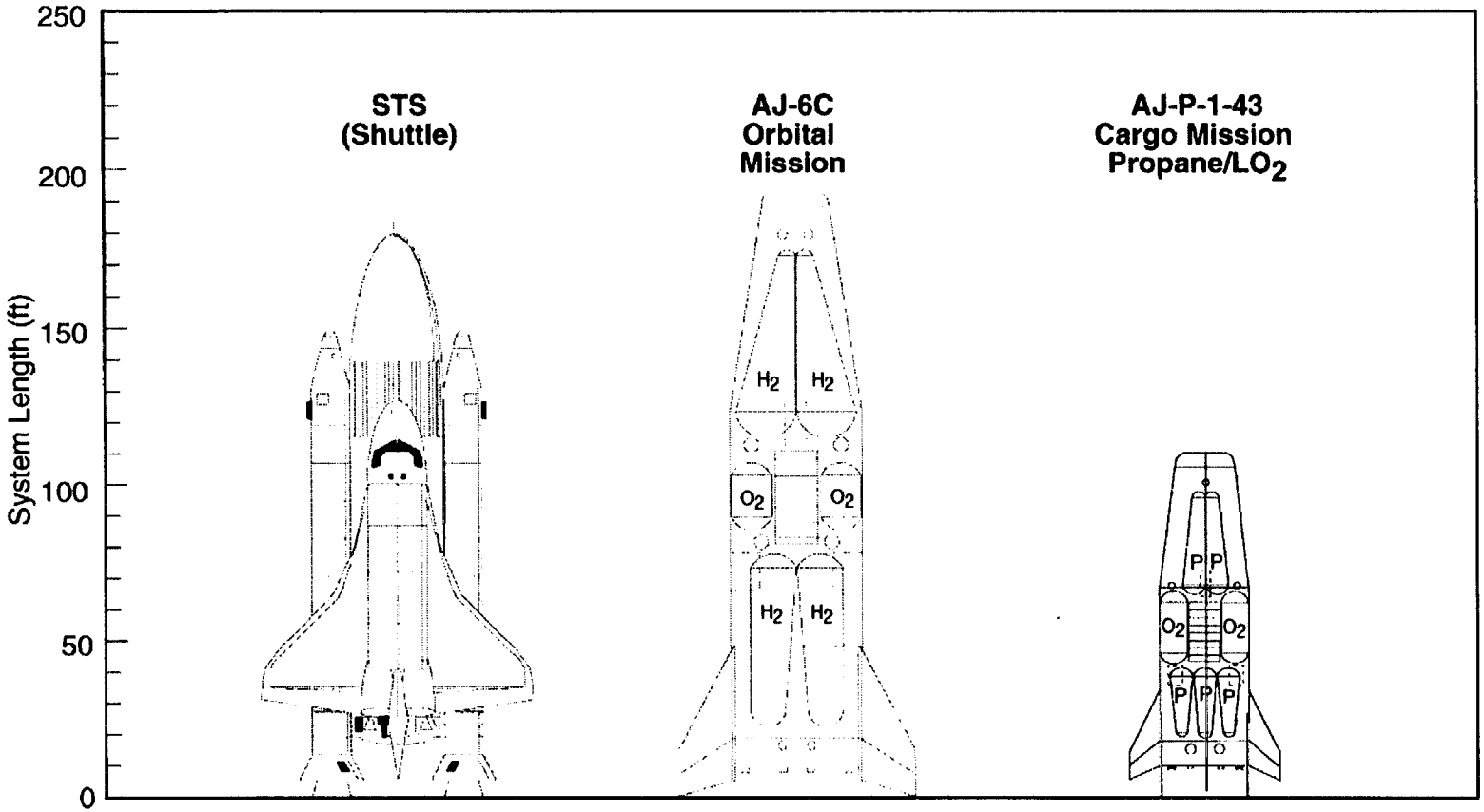

• Vehicle	Shuttle	SSTO/HTHL	HTHL
• Propulsion	Rocket	3 x RBCC	2 x RBCC
• GLOW (M lbm)	4.5	0.54	0.477
• Dry Mass (k lbm)	508	103	79
• Velocity (fps)	– –	30,750	26,900
• Thrust, L.O. (k lbf)	6,050	325	286
• Payload LEO (k lbm)	53.8	10–29	–
• Payload ISS (k lbm)	41	0–20	–

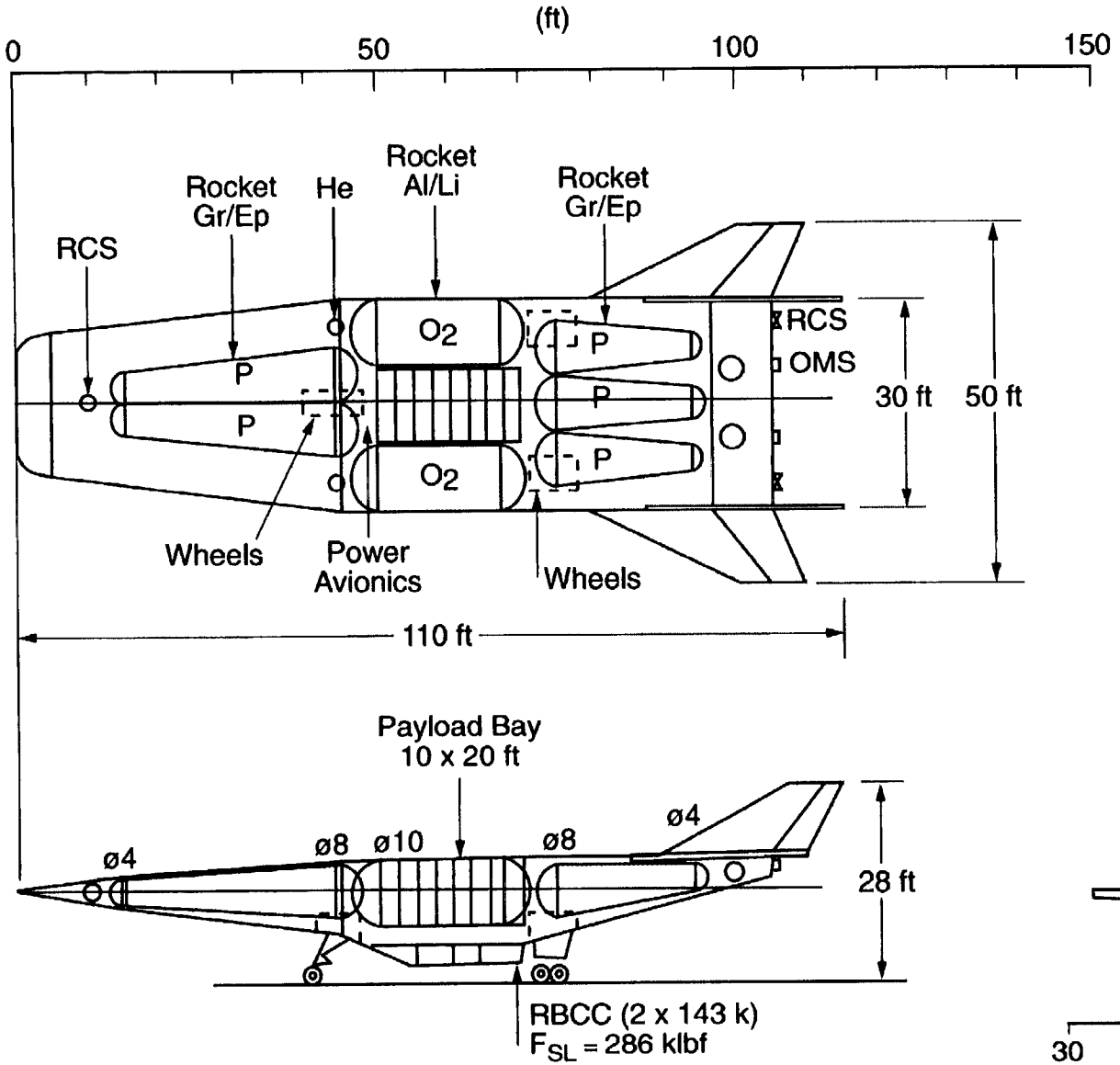

Case: AJ-P-1-43
M_T = 10 Mass (klb)

Paramater		NG	+G
• Payload	=	19	5
• W_{GTOM}	=	477	477
• W_{ignit}	=	506	506
• W_p use	=	373	373
• W dry	=	65	79
• W_p run	=	29	29
• Wp OMS	=	8	8
• λ_p	=	0.842	0.818
• T/W_o	=	0.6	
• T/W_{eng}	=	43:1	
• ΔV main	=	26,900 ft/sec	
• ΔV OMS	=	1,000 ft/sec	
• ΔV RCS	=	200 ft/sec	

A ref = 3000 ft^2
P = propane (C_2H_8) fuel

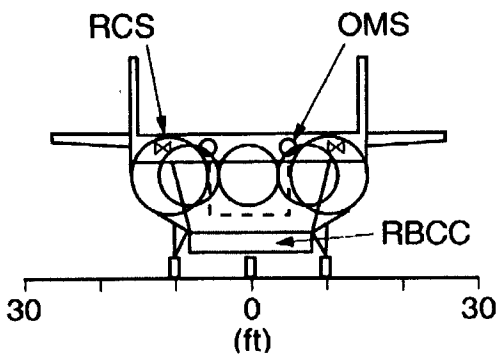

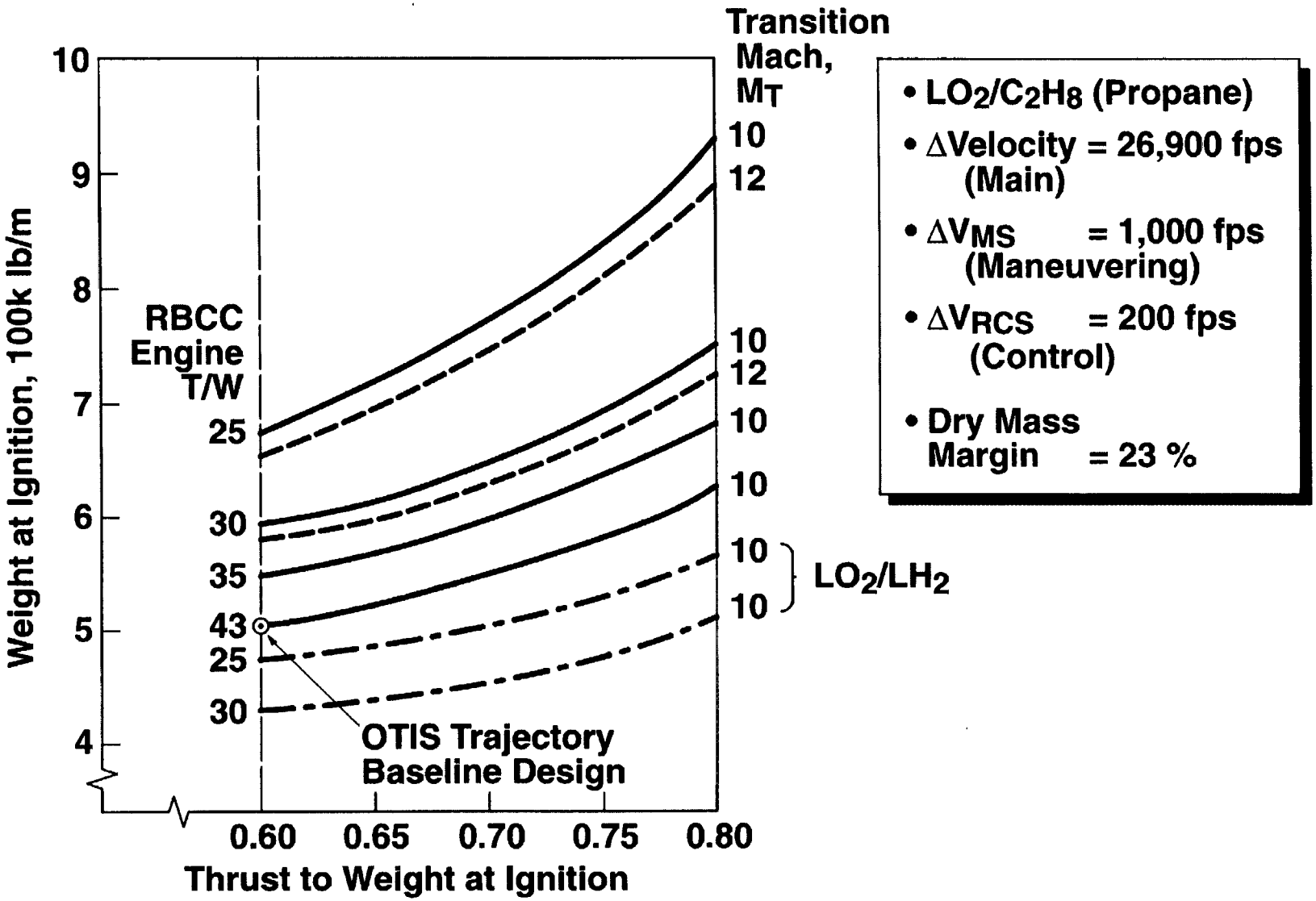
Transition Mach, M_T
10
12
10
12
10
10
10
10
LO_2/LH_2
RBCC Engine T/W
25
30
35
43
25
30
OTIS Trajectory Baseline Design
Weight at Ignition, 100k lb/m
10
9
8
7
6
5
4
0.60
0.65
0.70
0.75
0.80
Thrust to Weight at Ignition
• LO_2/C_2H_8 (Propane)
• ΔVelocity = 26,900 fps (Main)
• ΔV_{MS} = 1,000 fps (Maneuvering)
• ΔV_{RCS} = 200 fps (Control)
• Dry Mass Margin = 23 %

$T/W_0 = 0.6$
$T/W_e = 43:1$
$M_T = 10$
$S_{ref} = 6{,}800\ ft^2$ (aero)
$A_c = 255\ ft^2$ (RBCC)

Range (max) = 7,643 nmi
(14,154 km)
$Q_{max} = 2{,}000$ psf

Mission: Anchorage to
Brisbane or Singapore

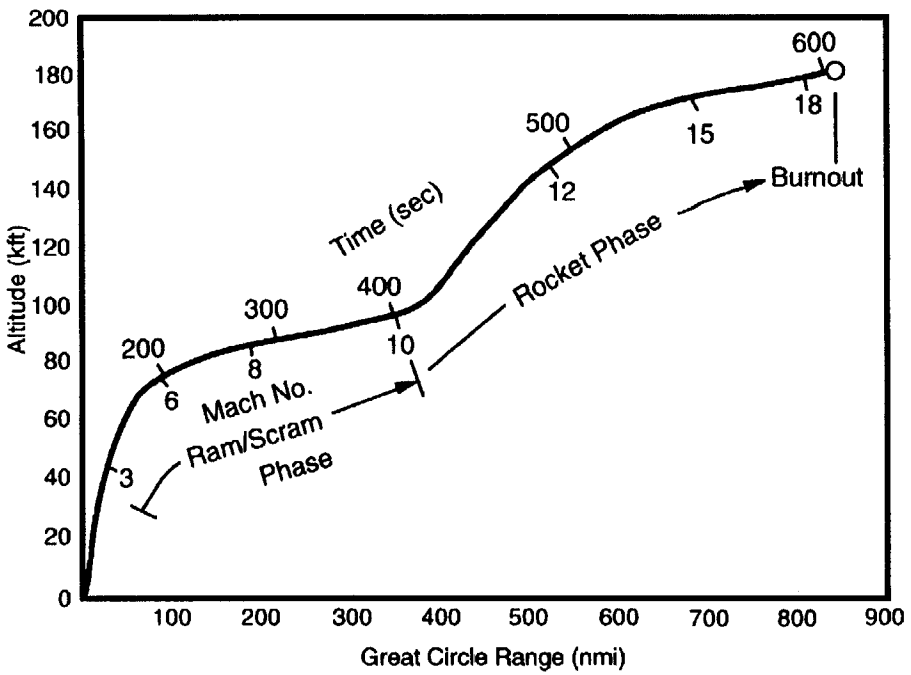

Parameter	Units	Launch	Burnout
• W_{GTOW}	lbm	477,267	103,521
• Q	psf	239	236
• Time	sec	0	610.3
• Altitude	ft	200	179,411
• Velocity	fps	450	20,523
• Gamma	deg	0.83	0.915
• Accel	g's	0.75	2.93
• Thrust	lbf	287,404	305,000
• Alpha	deg	17.2	7.32

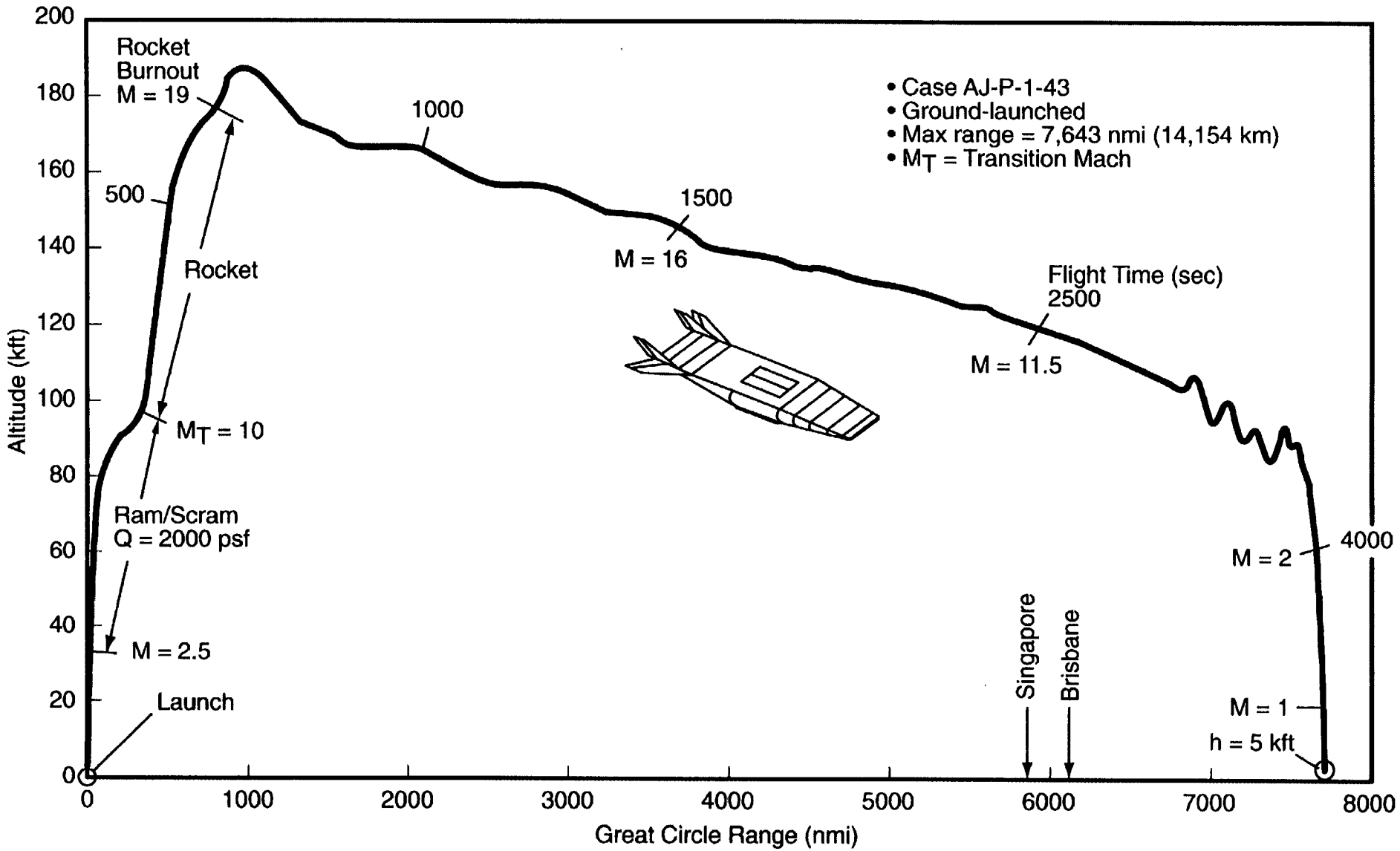
Rocket
Burnout
M = 19
1000
500
1500
M = 16
Rocket
Flight Time (sec)
2500
M = 11.5
M_T = 10
Ram/Scram
Q = 2000 psf
M = 2
4000
M = 2.5
Launch
Singapore
Brisbane
M = 1
h = 5 kft
• Case AJ-P-1-43
• Ground-launched
• Max range = 7,643 nmi (14,154 km)
• M_T = Transition Mach
Altitude (kft)
200
180
160
140
120
100
80
60
40
20
0
0
1000
2000
3000
4000
5000
6000
7000
8000
Great Circle Range (nmi)

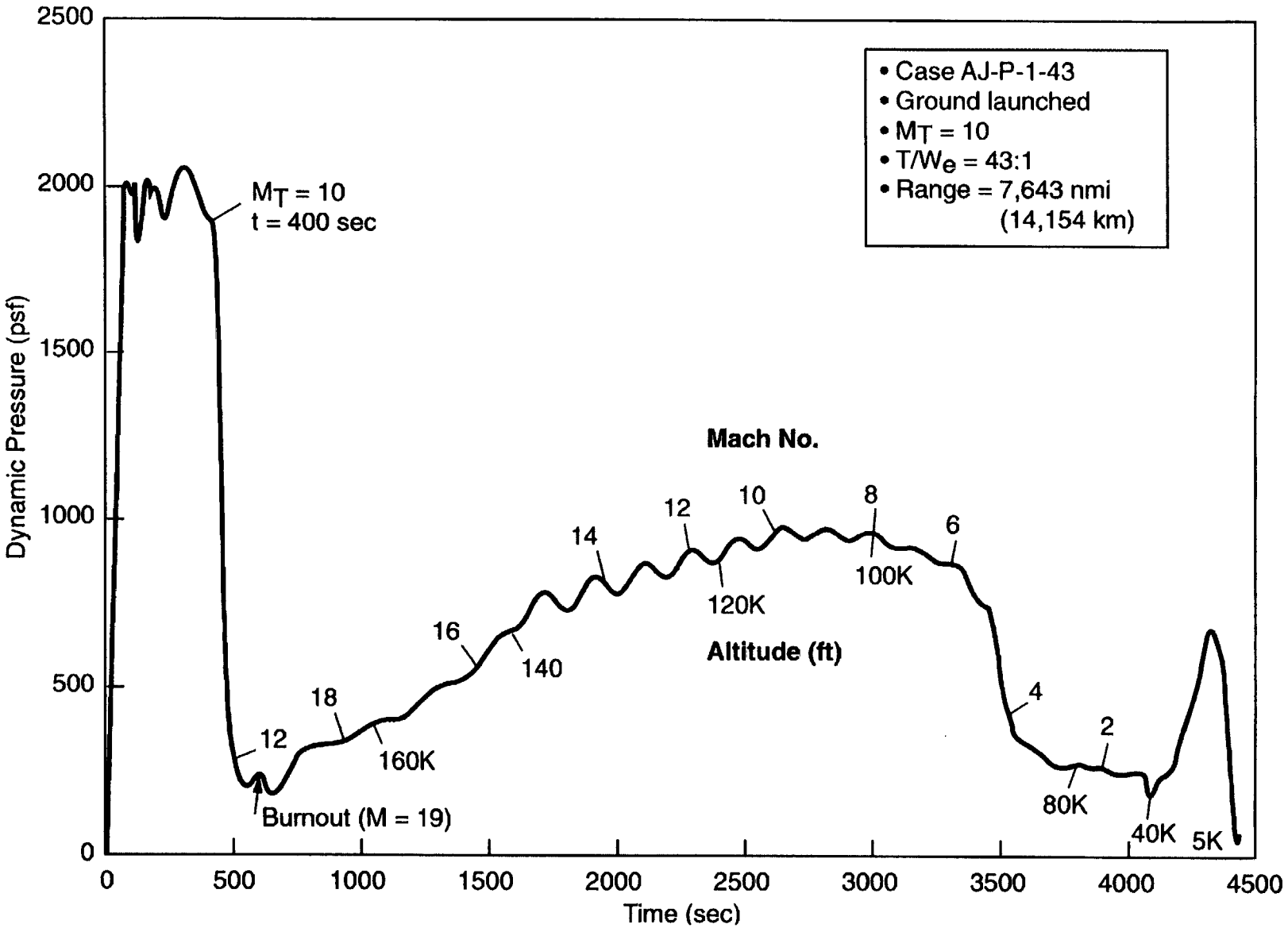
• Case AJ-P-1-43
• Ground launched
• MT = 10
• T/We = 43:1
• Range = 7,643 nmi
(14,154 km)
MT = 10
t = 400 sec
Mach No.
Altitude (ft)
Burnout (M = 19)
Dynamic Pressure (psf)
Time (sec)
0
500
1000
1500
2000
2500
3000
3500
4000
4500
12
18
160K
16
140
14
12
120K
10
8
100K
6
4
80K
2
40K
5K

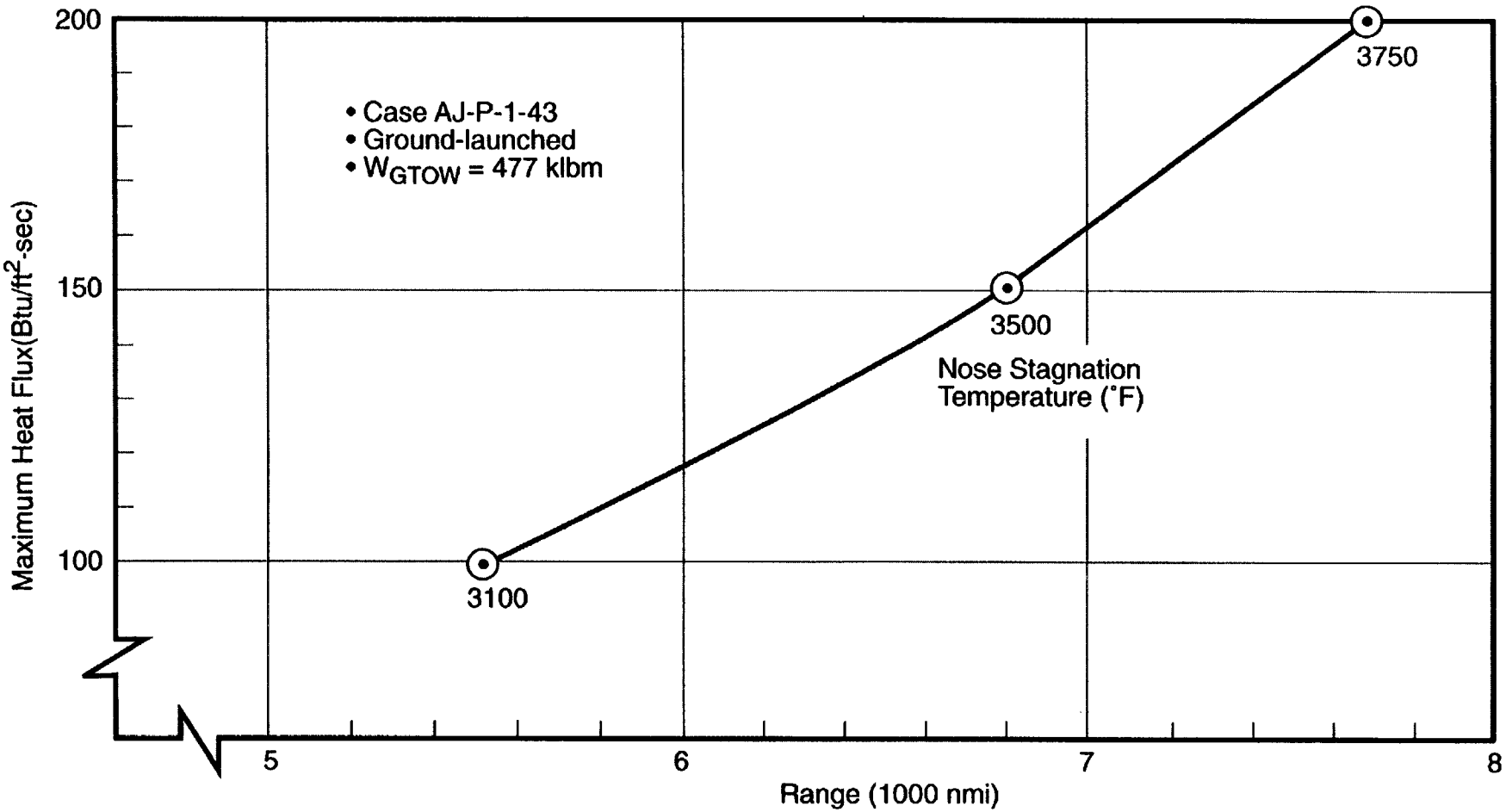
200
150
100
Maximum Heat Flux(Btu/ft2-sec)
• Case AJ-P-1-43
• Ground-launched
• WGTOW = 477 klbm
3750
3500
Nose Stagnation
Temperature (°F)
3100
5
6
7
8
Range (1000 nmi)

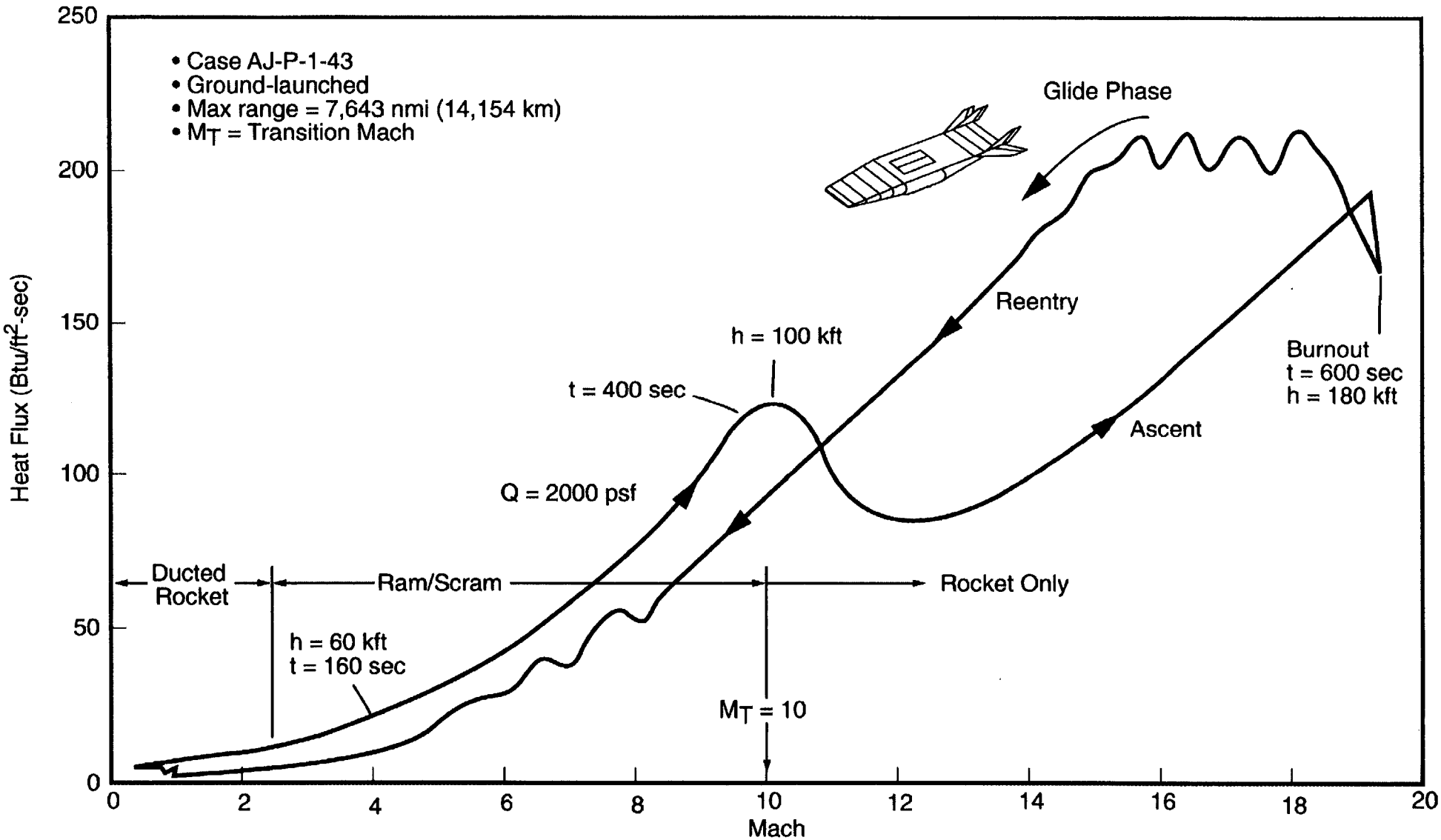
• Case AJ-P-1-43
• Ground-launched
• Max range = 7,643 nmi (14,154 km)
• M_T = Transition Mach
Glide Phase
Reentry
h = 100 kft
t = 400 sec
Burnout
t = 600 sec
h = 180 kft
Ascent
Q = 2000 psf
Ducted Rocket
Ram/Scram
Rocket Only
h = 60 kft
t = 160 sec
M_T = 10
Heat Flux (Btu/ft^2-sec)
Mach
0
50
100
150
200
250
0
2
4
6
8
10
12
14
16
18
20

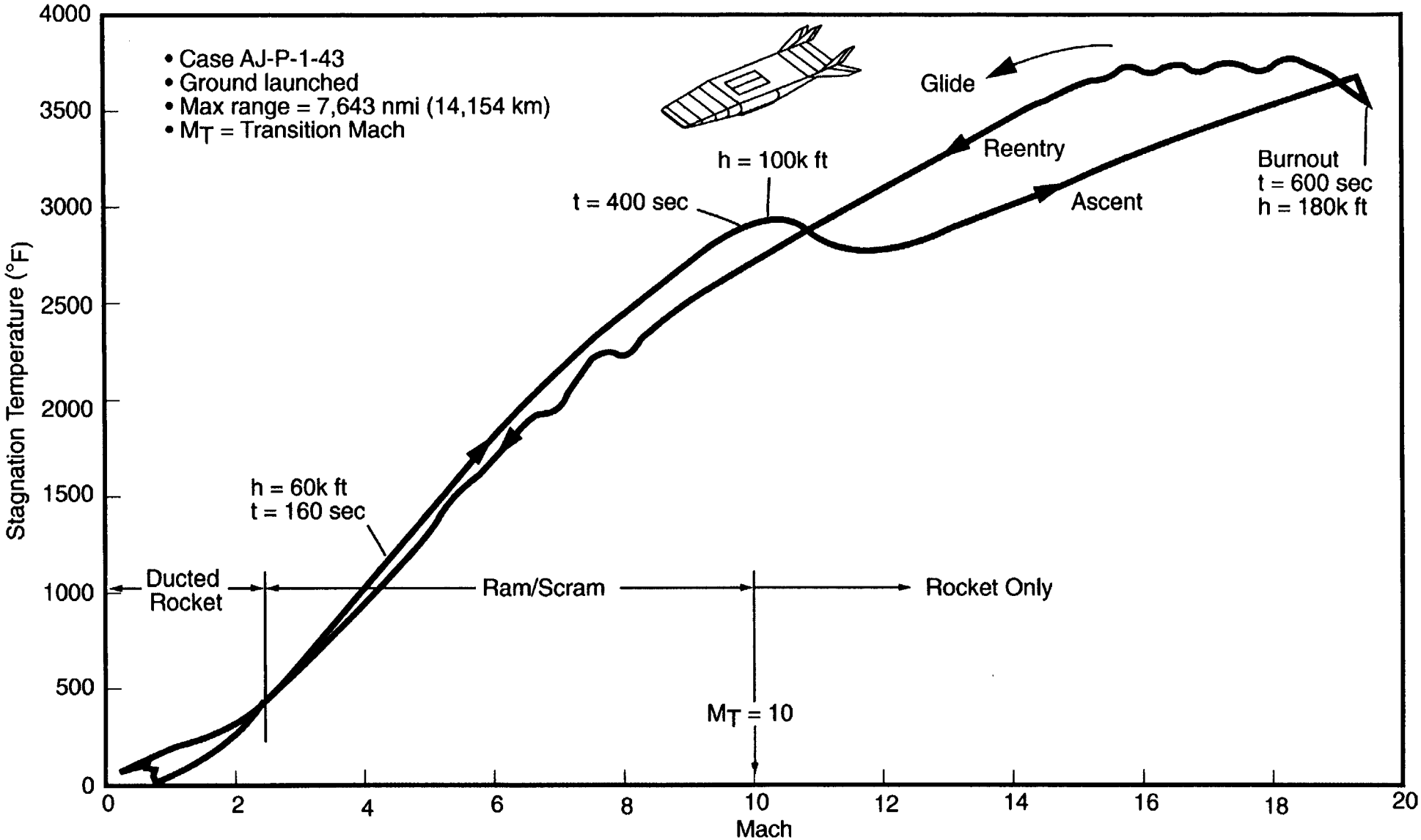
• Case AJ-P-1-43
• Ground launched
• Max range = 7,643 nmi (14,154 km)
• M_T = Transition Mach
Glide
Reentry
Ascent
h = 100k ft
t = 400 sec
Burnout
t = 600 sec
h = 180k ft
h = 60k ft
t = 160 sec
Ducted Rocket
Ram/Scram
Rocket Only
M_T = 10
Stagnation Temperature (°F)
Mach
4000
3500
3000
2500
2000
1500
1000
500
0
0
2
4
6
8
10
12
14
16
18
20

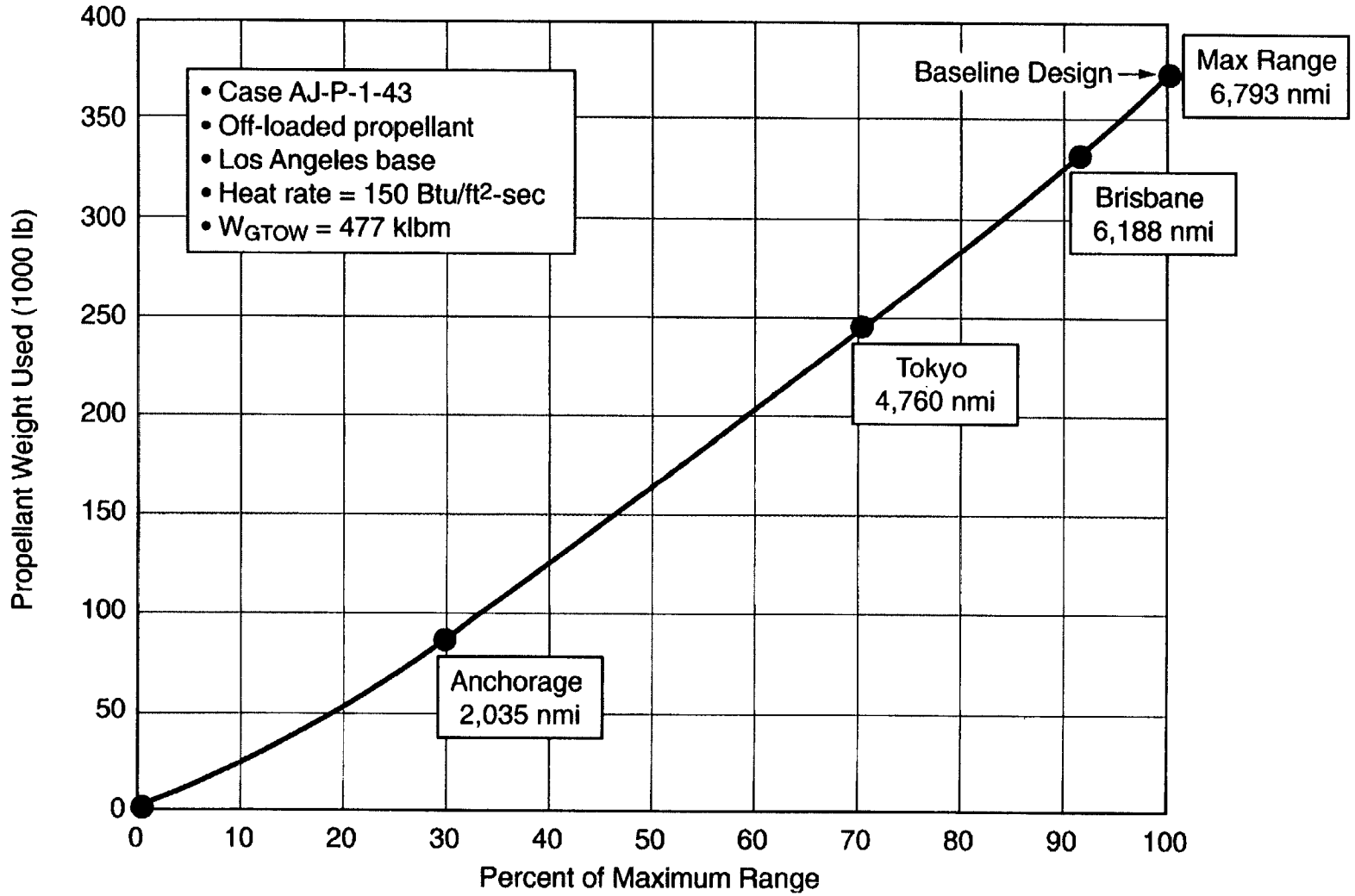
• Case AJ-P-1-43
• Off-loaded propellant
• Los Angeles base
• Heat rate = 150 Btu/ft2-sec
• WGTOW = 477 klbm
Baseline Design
Max Range
6,793 nmi
Brisbane
6,188 nmi
Tokyo
4,760 nmi
Anchorage
2,035 nmi
Propellant Weight Used (1000 lb)
400
350
300
250
200
150
100
50
0
0
10
20
30
40
50
60
70
80
90
100
Percent of Maximum Range

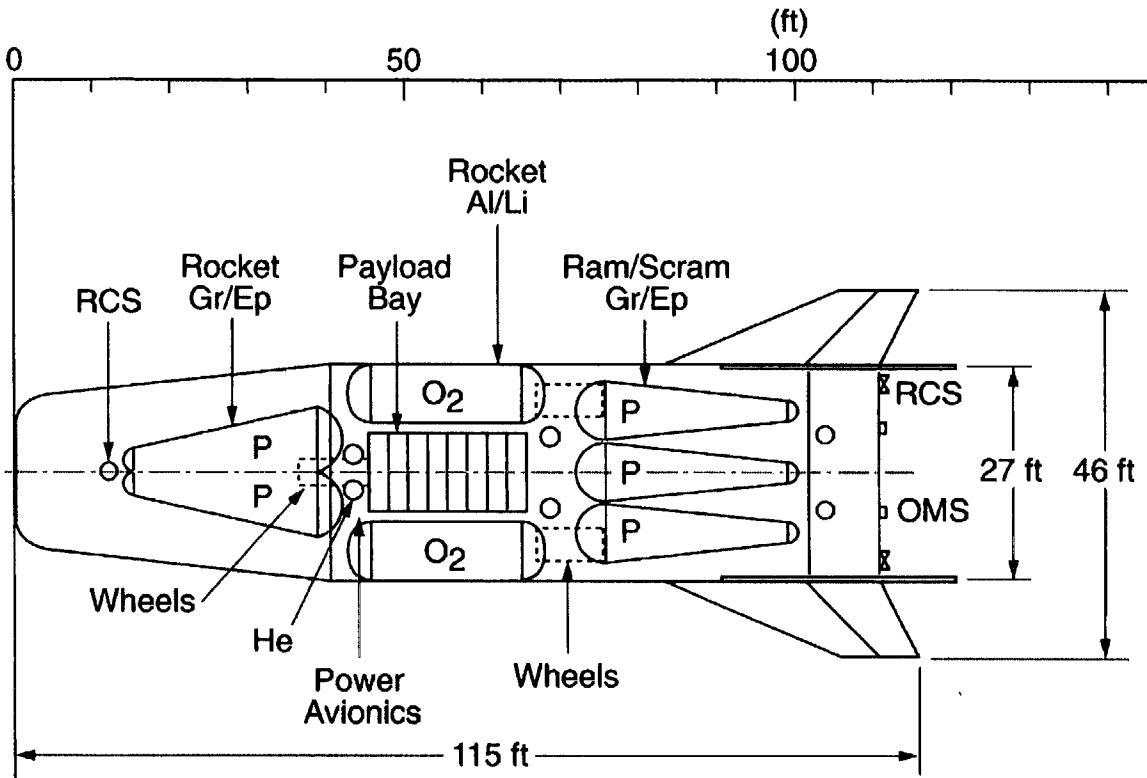

Case: AJ-P-6-AL
M_T = 10

Mass (klb)

Paramater		NG	+G
• Payload	=	18	5
• W_{GTOM}	=	390	390
• W_p use	=	290	290
• W dry	=	64	77
• Wp OMS	=	8	8
• λ_p	=	0.801	0.773
• T/W_o	=	1.0	
• T/W_{eng}	=	35:1	
• ΔV main	=	23,900 fps	
• ΔV OMS	=	1,000 fps	
• ΔV RCS	=	200 fps	

A ref = 3000 ft^2
P = propane (C_2H_8) fuel

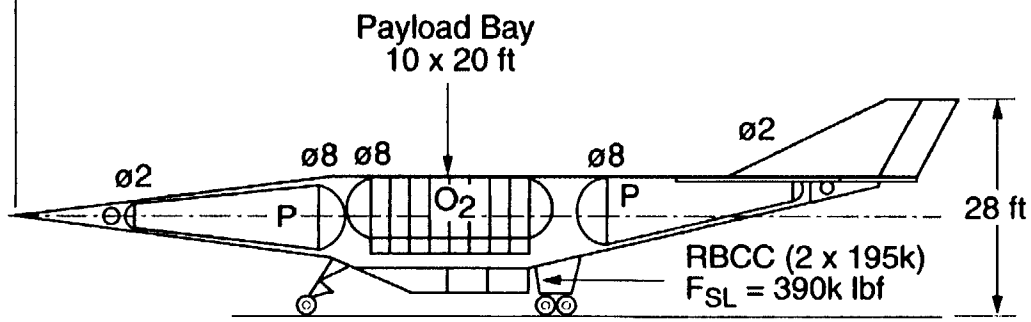

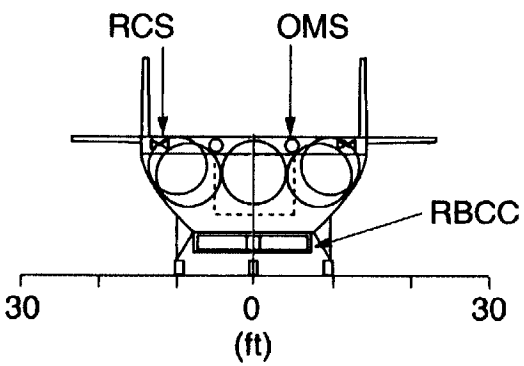

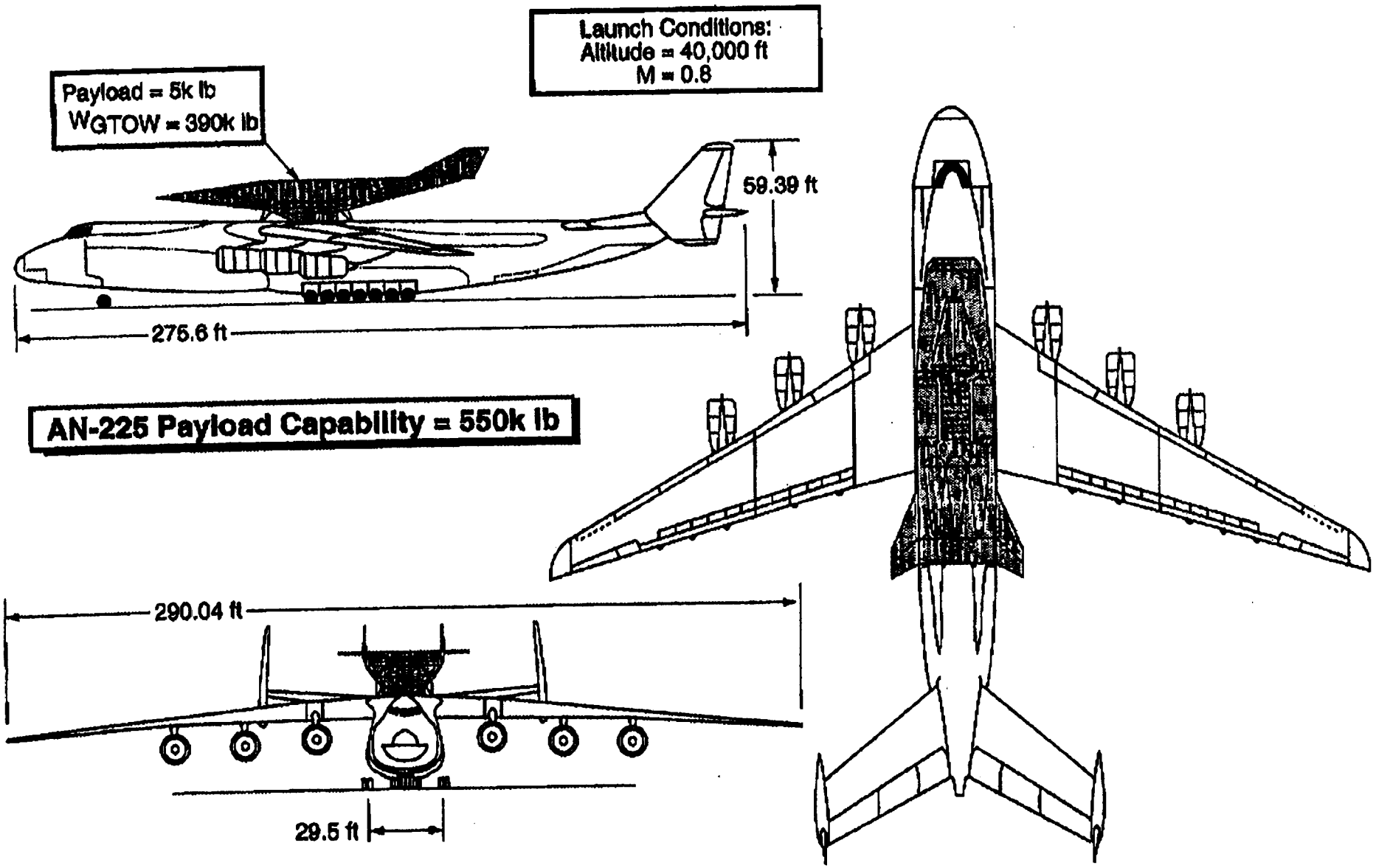

(18)
Fig. 46 48 47

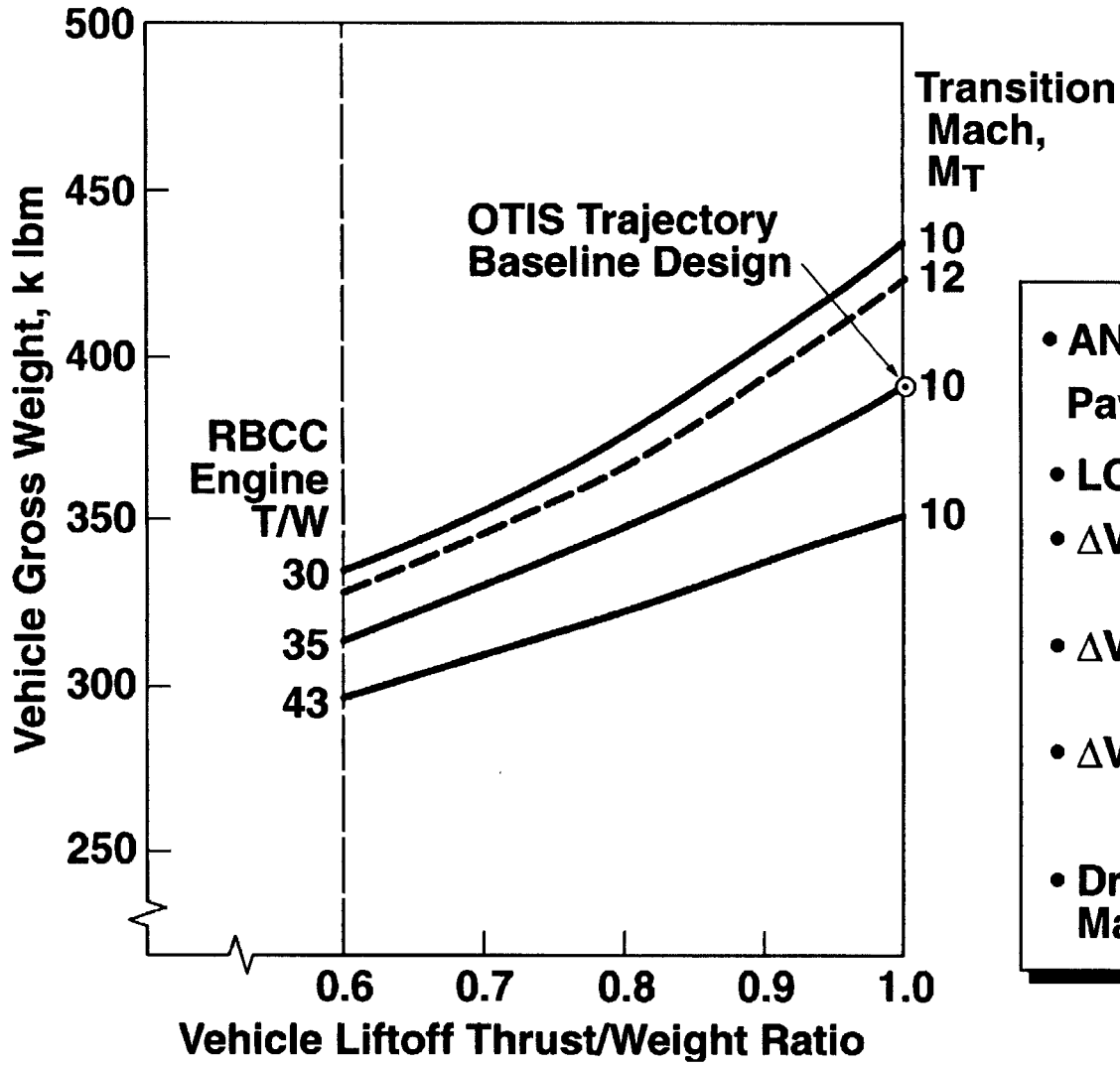

- AN-225 Launch Aircraft Payload Limit = 550k lbm
- LO_2/C_2H_8 (Propane)
- ΔVelocity = 23,900 fps (Main)
- ΔV_{MS} = 1,000 fps (Maneuvering)
- ΔV_{RCS} = 200 fps (Control)
- Dry Mass Margin = 23 %

- $T/W_o = 1.0$
- $T/W_e = 35$
- $M_T = 10$
- $S_{ref} = 6800\ ft^2$ (Aero)
- $A_c = 255\ ft^2$ (RBCC)
- Range (Maximum) = 7,694 nmi (14,248 km)
- $Q_{max} = 2000$ psf
- Mission: Anchorage to Singapore

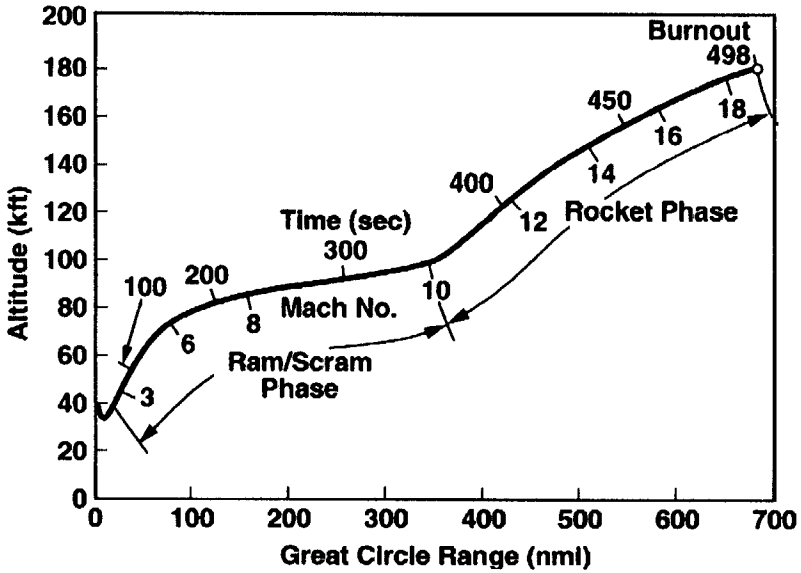

Parameter	Units	Launch	Burnout
W_{GTOW}	lbm	390,274	100,362
Q	psf	175	222
Time	sec	0	498
Altitude	ft	40,000	181,240
Velocity	fps	775	20,583
Gamma	deg	0.83	1.554
Accel	g	1.08	3.0
Thrust	lbf	389,698	299,944
Alpha	deg	17.2	4.6

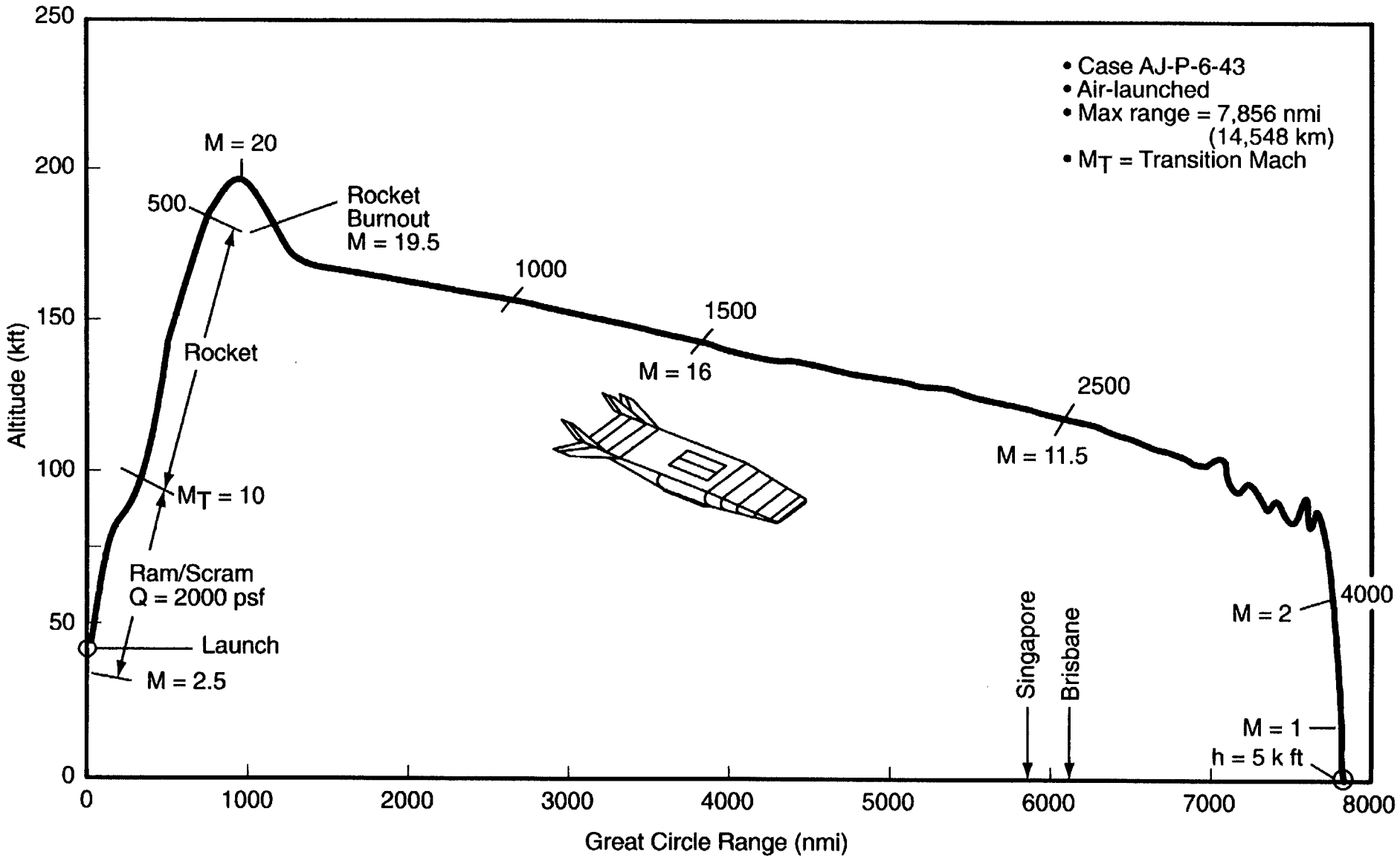
• Case AJ-P-6-43
• Air-launched
• Max range = 7,856 nmi
(14,548 km)
• M_T = Transition Mach
M = 20
500
Rocket
Burnout
M = 19.5
1000
1500
M = 16
2500
M = 11.5
4000
M = 2
Rocket
M_T = 10
Ram/Scram
Q = 2000 psf
Launch
M = 2.5
Singapore
Brisbane
M = 1
h = 5 k ft
Altitude (kft)
250
200
150
100
50
0
0
1000
2000
3000
4000
5000
6000
7000
8000
Great Circle Range (nmi)

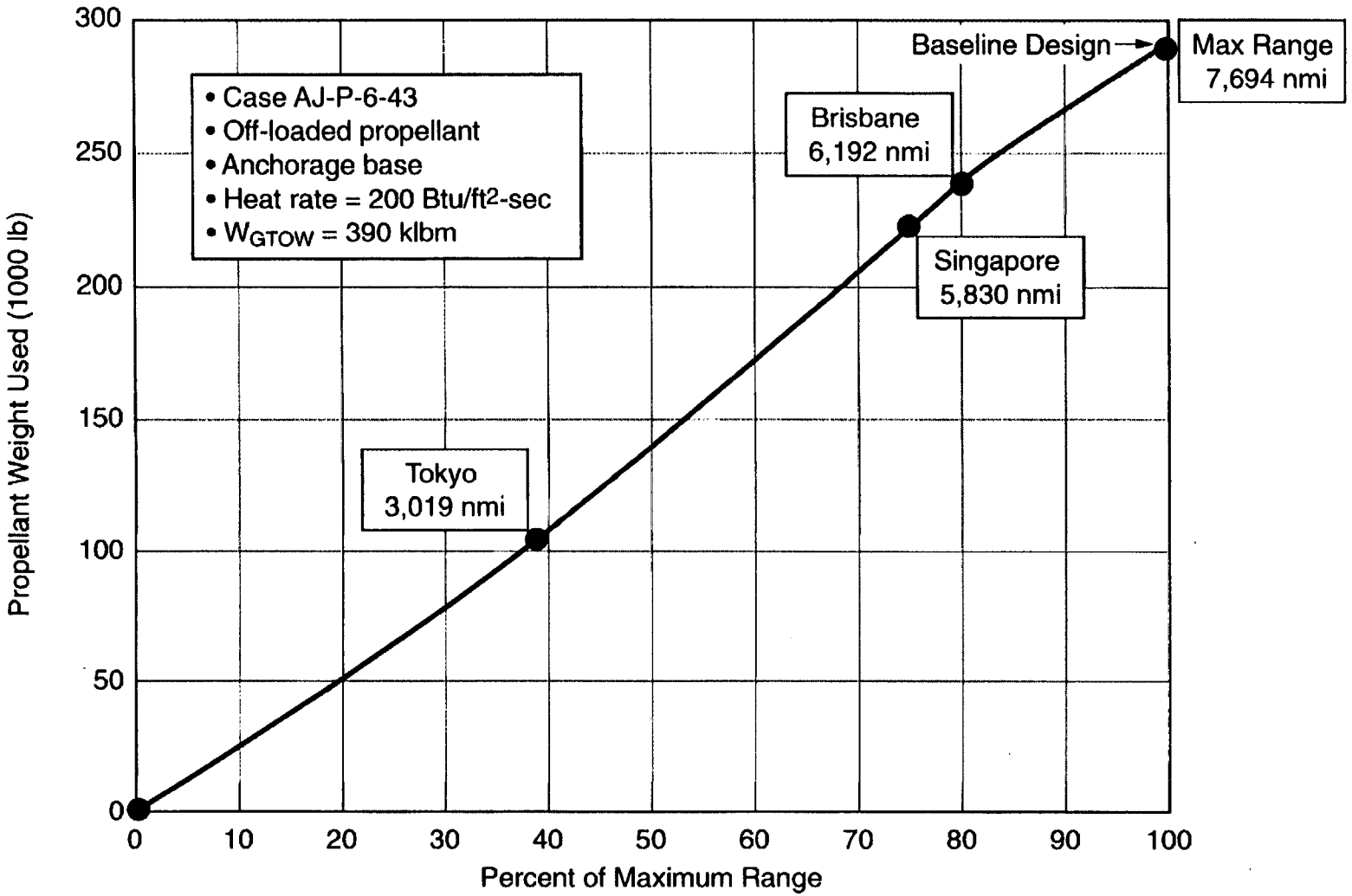
Propellant Weight Used (1000 lb)
300
250
200
150
100
50
0
0
10
20
30
40
50
60
70
80
90
100
Percent of Maximum Range
• Case AJ-P-6-43
• Off-loaded propellant
• Anchorage base
• Heat rate = 200 Btu/ft2-sec
• WGTOW = 390 klbm
Baseline Design
Max Range
7,694 nmi
Brisbane
6,192 nmi
Singapore
5,830 nmi
Tokyo
3,019 nmi